NUREG/CR-3724
SAND84-0660
R1, RD
Printed July 1984

# Ultimate Strength Analyses of the Watts Bar, Maine Yankee, and Bellefonte Containments

J. Jung

Prepared by
Sandia National Laboratories
Albuquerque, New Mexico 87185 and Livermore, California 94550
for the United States Department of Energy
under Contract DE-AC04-76DP00789

Prepared for
U. S. NUCLEAR REGULATORY COMMISSION

Available from

GPO Sales Program
Division of Technical Information and Document Control
U.S. Nuclear Regulatory Commission
Washington, D.C. 20555

and

National Technical Information Service
Springfield, Virginia 22161

NUREG/CR-3724
SAND84-0660
R1 and RD

# ULTIMATE STRENGTH ANALYSES OF THE WATTS BAR, MAINE YANKEE, AND BELLEFONTE CONTAINMENTS

J. Jung

Date Published: July 1984

Sandia National Laboratories
Albuquerque, NM 87185
Operated by
Sandia Corporation
for the U.S. Department of Energy

Prepared for
Division of Accident Evaluation
Office of Nuclear Regulatory Research
U. S. Nuclear Regulatory Commission
Washington, DC
Under Memorandum of Understanding DOE 40-550-75
NRC FIN NO. A1258

## ABSTRACT

As part of Sandia National Laboratories' Severe Accident Sequence Analysis (SASA) Program, structural analyses of the Watts Bar, Maine Yankee, and Bellefonte containment structurres were performed with the objective of obtaining realistic estimates of their ultimate static pressure capacities. The Watts Bar investigation included analyses of the containment shell, equipment hatch, anchorage systems, and personnel lock. The ultimate pressure capability is estimated to be between 120 and 137 psig, corresponding to shell yielding and equipment hatch buckling, respectively. The Maine Yankee investigation consisted of an analysis of the containment shell and estimated its failure pressure to be between 96 and 118 psig. For the Bellefonte containment, analyses of the containment shell and equipment hatch were performed. The pressure capacity of the Bellefonte containment is estimated to be between 130 and 139 psig, corresponding to dome tendon yielding and cylinder wall tendon yielding, respectively.

Table of Contents

## List of Figures

## List of Tables

## INTRODUCTION

Probabilistic risk assessments have shown that risk from nuclear power reactors is dominated by severe accidents, that is, accidents in which substantial damage is sustained by the reactor core. Radiological consequences from severe accidents can range from minor to major, depending on a number of factors including the degree to which radionuclides released from the core are retained within containment. Sandia Laboratories has undertaken, as part of the Severe Accident Sequence Analysis (SASA) Program, a systematic study of PWR containment loadings that could affect containment integrity during such accidents. The SASA objectives are to determine what events threaten containment integrity, the timing of these events, the uncertainties in both of the former, and the efficiency of operator mitigation actions. To accomplish these objectives containment performance information is needed that includes the structural response of containments when subjected to severe accident induced loadings.

This report covers structural analyses of the Watts Bar, Maine Yankee, and Bellefonte containment structures. These analyses, performed as part of the SASA Program, provide realistic estimates of the ultimate static pressure capabilities of these containments. The three containments considered represent a cross-section of different PWR containment types. The Watts Bar containment is a hybrid steel type, the Maine Yankee containment is a steel lined reinforced concrete building, and the Bellefonte containment is a steel lined prestressed concrete structure.

## WATTS BAR CONTAINMENT ANALYSES

Structural analyses of the following containment components were performed:

1. The containment shell without penetrations,
2. The equipment hatch,
3. The containment anchorage system, and
4. The personnel lock.

These components were believed to be the most susceptible to early failure due to internal pressurization and also are the most amenable to analysis.

Because the objective of the analyses was to obtain a realistic estimate of the ultimate capacity of the containment structure and since it is generally believed that the true ultimate capacity of a typical steel containment is beyond that of initial yielding, analysis techniques which are valid for loadings beyond the initial yielding of the material were used. The finite element analyses conducted were performed with either the MARC [1] or ABAQUS [2] finite element computer codes. Both of these codes have large deformations and finite (large) strain capabilities. These two effects may have significant contributions to the analysis results due to the large ductility of most steel structures. The estimates of the ultimate capacity of the material were based on a maximum von Mises equivalent stress criteria that helps to account for the multiaxial stress state of the containment material[3].

To obtain as realistic results as possible, actual (as-built) material properties were used for the analyses. With the cooperation of the Tennessee Valley Authority, a sampling of the mill test reports for the materials used in the Watts Bar Unit 1 containment was used to compute the average properties used in these analyses. This data is given in Appendix A and is summerized in Table 1. The use of these properties is discussed in the sections covering the analysis of each component.

## Containment Shell Analysis

### Description of the Containment Structure

The Watts Bar containment structure [4] is a stiffened steel shell consisting of a cylindrical wall, hemispherical dome, and a bottom liner plate encased in concrete. Figure 1 shows the general configuration and the plate sizes used for the structure. The design pressure for the containment is 13.5 psig.

The structure is composed of side walls measuring 111 feet, 8-5/8 inches high from the top of the concrete base to the spring line of the dome and has an inside diameter of 115 feet. The bottom liner plate is 1/4 inches thick. The cylinder thickness varies from 1-3/8 inches at the bottom to 1-1/2 inches at the spring line. The dome thickness varies from 1-3/8 inches to 13/16 inches and is 15/16 inches thick at the apex. The entire containment structure is constructed of A516-GR70 steel.

### Finite Element Model and Material Properties

An axisymmetric elastic-plastic finite element analysis of the Watts Bar containment shell was performed using the computer

Table 1

Summary of Watts Bar Material Properties

| Component | # Samples | Yield Stress* (ksi) | | Ultimate Stress* (ksi) | | Elongation* (%) | |
|---|---|---|---|---|---|---|---|
| Cylindrical Shell Plate | 25 | 45.9 | (3.07) | 74.2 | (2.51) | 29.5 | (3.68) |
| Dome Plate | 32 | 46.3 | (5.35) | 74.8 | (3.17) | 27.7 | (3.06) |
| Personnel Lock | 1 | 50.7 | | 73.4 | | 22.0 | |
| Equipment Hatch | 6 | 50.2 | (1.78) | 77.9 | (4.29) | 24.8 | (4.92) |
| Tie Down Bolts | 10 | 115.7 | (2.92) | 136.8 | (1.64) | 19.4 | (0.77) |

*The first number is the average value and the second is the standard deviation.

program MARC. Only the containment shell was modeled using a fixed base boundary condition. Because steel structures are usually ductile, the large displacement and finite strain capabilities of the program were utilized.

The model, Figure 2, consisted of 62 nodes and 49, two noded axisymmetric shell elements. The containment shell and circumferential stiffeners were represented in the analytical model. The loading was a static internal pressure and was incrementally applied.

The steel true stress-true strain curve used for the analysis is shown in Figure 3. The elastic portion of the curve does not appear due to the scaling necessary to show the strain hardening portion of the curve. This curve was constructed by taking the average yield and ultimate strength valves from the sampling of the actual material properties (Appendix A) and then fitting the general shape of the curve to other stress-strain curves for A516-GR70 steel. The engineering stress-strain curve was then converted to a true stress-true strain curve. The most important aspect of the fitting procedure was the use of approximately 13% engineering strain as the point where the ultimate stress was reached. The 13% strain value corresponded to the ultimate stress in the engineering stress strain curves of A516-GR70 steel that were available.

The criteria for failure of the shell was based on a maximum von Mises equivalent stress criteria.* Biaxial tests [3] of A516 GR70 material have shown that this criteria describes the failure surface well. After adjusting shell and dome ultimate strength data (Appendix A) to true stress the average value for the maximum equivalent stress is about 85 ksi.

Results of Analysis

The finite element analysis was conducted by incrementally increasing the internal pressure in the containment. An extra equlibrium iteration was imposed at each load step to keep the residual forces low.

---

*Von Mises equivalent stress in terms of principal stresses for the biaxial case is given by the expression:

$$\sigma_{eq} = [(\sigma_1)^2 + (\sigma_2)^2 + \sigma_1\sigma_2]^{1/2}$$

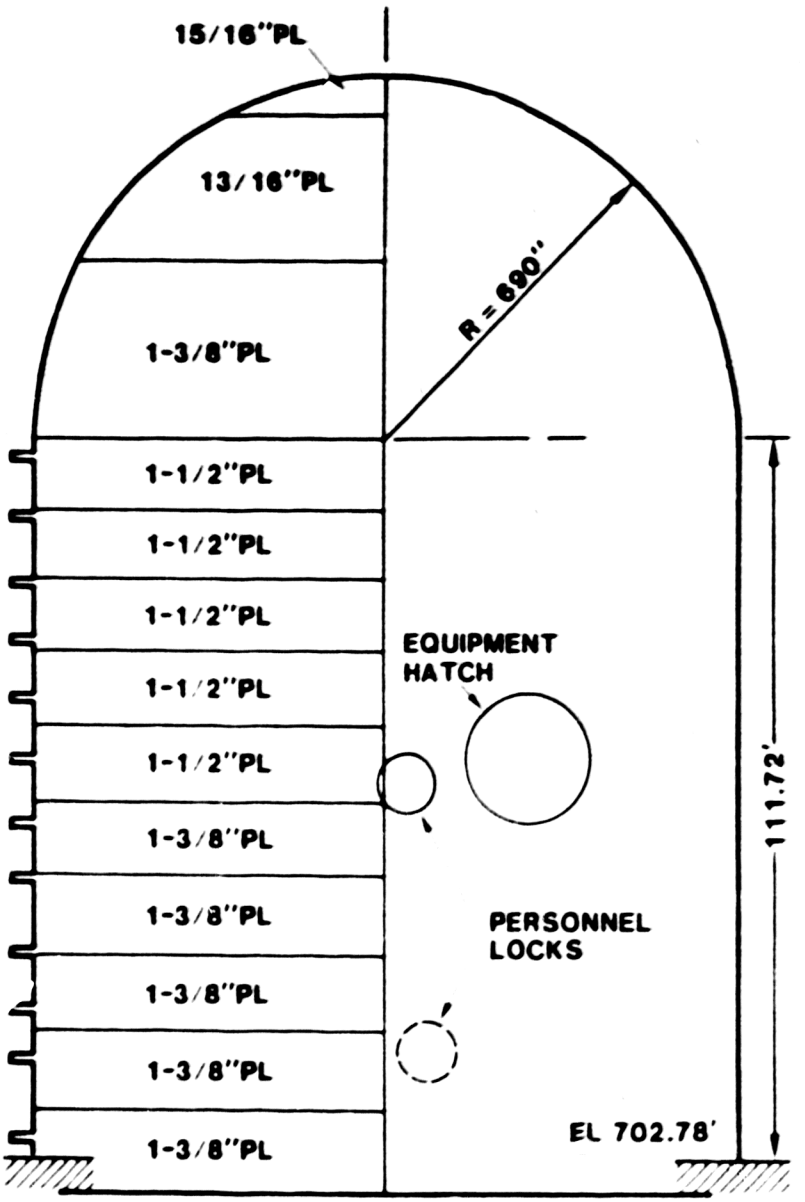


Figure 1

Watts Bar Steel Containment Vessel

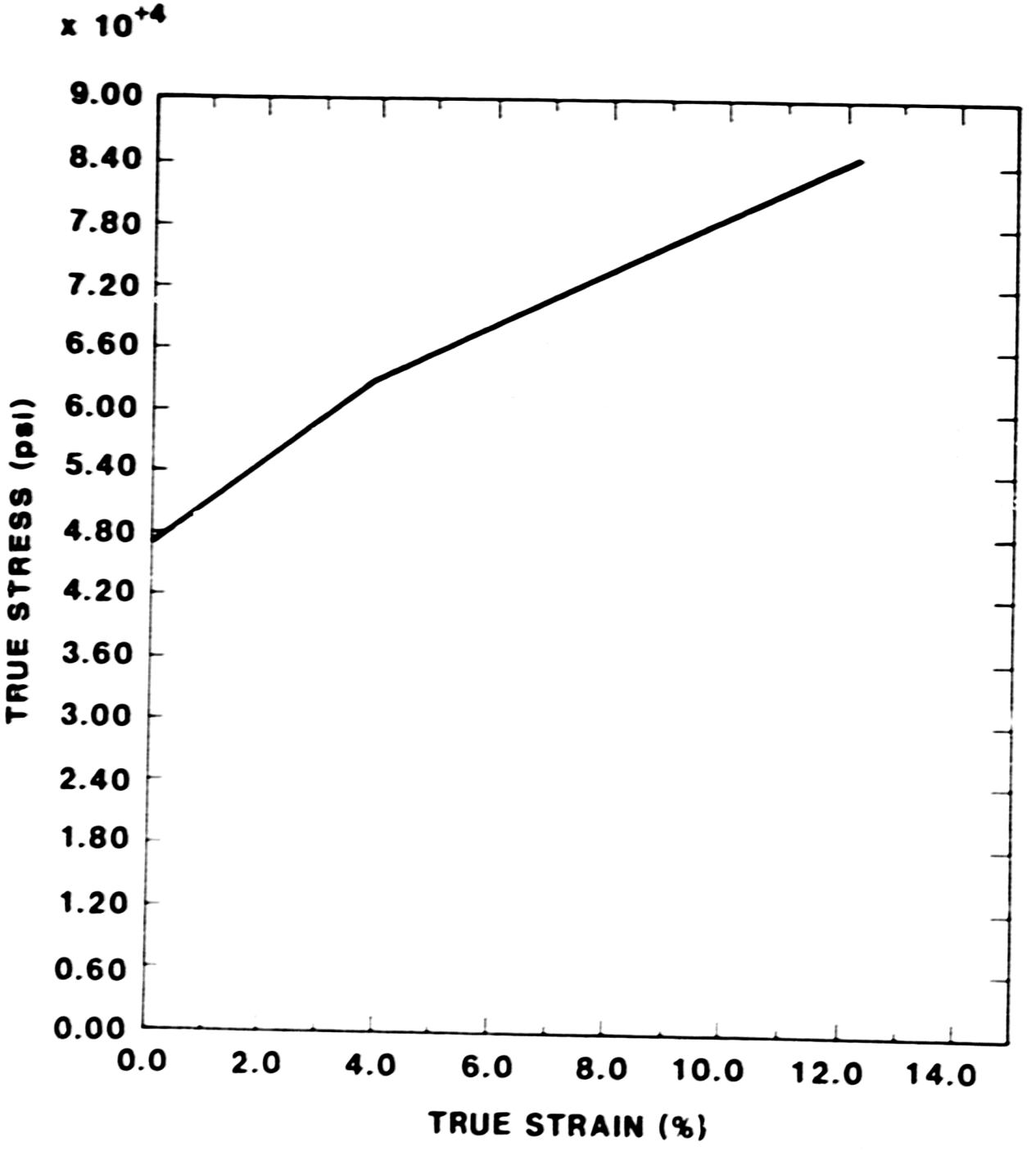


Figure 3

True Stress - True Strain Curve for
the Containment Shell Material

The finite element computer code, ABAQUS, was selected for the analyses because of its automatic load incrementation procedures, which are particularly well suited for buckling type problems. The analyses incorporated large deformation, elastic-plastic behavior.

A number of equipment hatch door boundary conditions were considered but the most realistic boundary condition was believed to be a roller condition (radial displacement allowed but no rotation allowed) on the outside equipment hatch tension ring. Other configurations and boundary conditions such as the inclusion of the sleeve were analyzed, but rejected as unrealistic because TVA engineers believe that the twenty 1-1/4 inch bolts cannot be expected to provide the necessary forces to maintain continuity between the sleeve and hatch at high pressures.

The equipment hatch analysis was treated as an axisymmetric problem using 33 three-noded axisymmetric shell elements. The geometry of the model and element boundaries are shown in Figure 9. The loading was a pressure applied to the inside surface of the equipment hatch.

### Finite Element Results

The finite element analysis results showed that there would be significant yielding of the equipment hatch tension ring and spherical door adjacent to the ring before buckling occurs at 137 psig. A displaced shape plot of the structure at approximately 137 psig is shown in Figure 10. This analysis neglects any imperfections in the door, which would lower the buckling pressure. It is interesting to note that an elastic eigenvalue analysis, based on equipment hatch's original geometry, yields a buckling load of 238 psig. The eigenvalue analysis overestimates the buckling load because the door's stiffness changes significantly as the material becomes plastic.

## Analysis of the Containment Anchorage System

### Description of the Anchorage System

The Watts Bar anchorage system, Figure 11, consists of two rows of 3-1/2-inch diameter bolts (minimum diameter of 3.338 inches) spaced approximately every two degrees. Each bolt has an initial preload of 444 kips.

**Analysis of Anchorage System**

From the reaction forces at the base of the containment (given by the containment shell finite element analysis) the loads on the tie-down bolts and their ultimate capacities were estimated.

For this analysis, it was assumed that the total reaction loads are carried by the tie-down bolts and the bolts' preloads were overcome [5]. The containment internal pressure at which yielding first occurs was determined. The average yield stress of the bolts is 116,000 psi and the average ultimate strength value is 137,000 psi, Appendix A.

First yielding of the bolts was found to occur at an internal pressure of approximately 172 psig. At this load, the following total reaction forces and moment are present (from the axisymmetric containment analysis):

| | | | |
|---|---|---|---|
| Axial force | = | $2.57 \times 10^8$ | lbs. |
| Radial shear | = | $6.06 \times 10^7$ | lbs. |
| Moment | = | $6.39 \times 10^8$ | in.-lbs. |

The maximum axial stress on a bolt is a combination of the applied axial stress and the stress due to the bending moment:

$$\frac{2.57 \times 10^8 (\text{lb})}{360 \ (\#\ \text{bolts})} \times \frac{1}{8.75\ (\text{sq. in.})} + \frac{6.39 \times 10^8 (\text{in-lb})}{13.375\ (\text{in.})}$$

$$\times \frac{1}{180\ (\text{bolts})} \times \frac{1}{8.75\ (\text{sq. in})} = 1.11 \times 10^5 \ \text{psi}$$

The shear stress in a bolt can be approximated by dividing the total shear load by the cross sectional area of the bolt:

$$\text{tau} = \frac{6.06 \times 10^7 \ \text{lb}}{360 \times 8.75\ (\text{sq. in.})} = 19{,}240 \ \text{psi}$$

Combining the axial and shear components yields an equivalant von Mises stress of 116,700 psi which is slightly greater than the mean yield stress of the bolts.

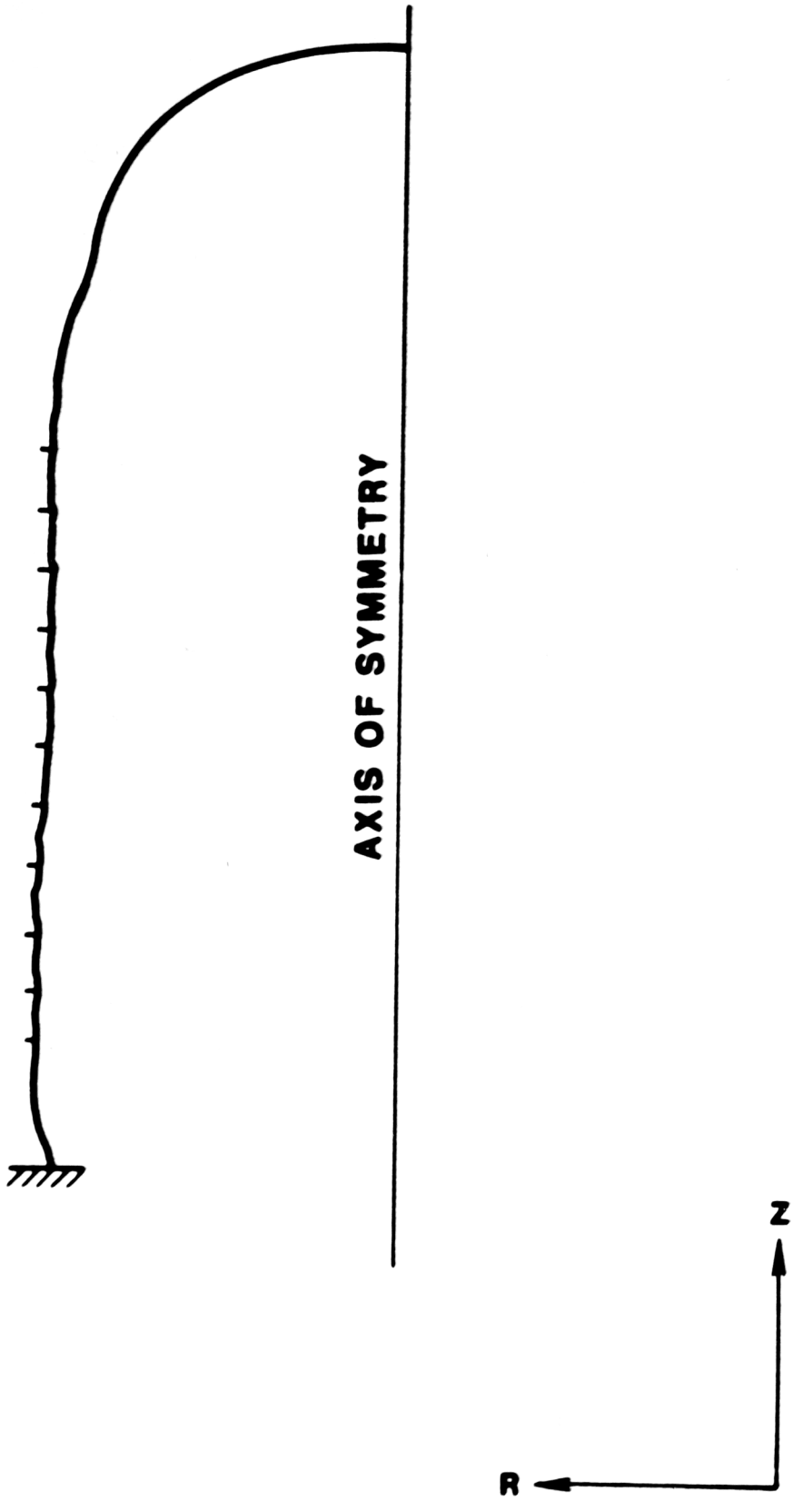


Figure 4

Displaced Shape of the Watts Bar Containment at 130 psig
(Displacement magnification of 10 x)

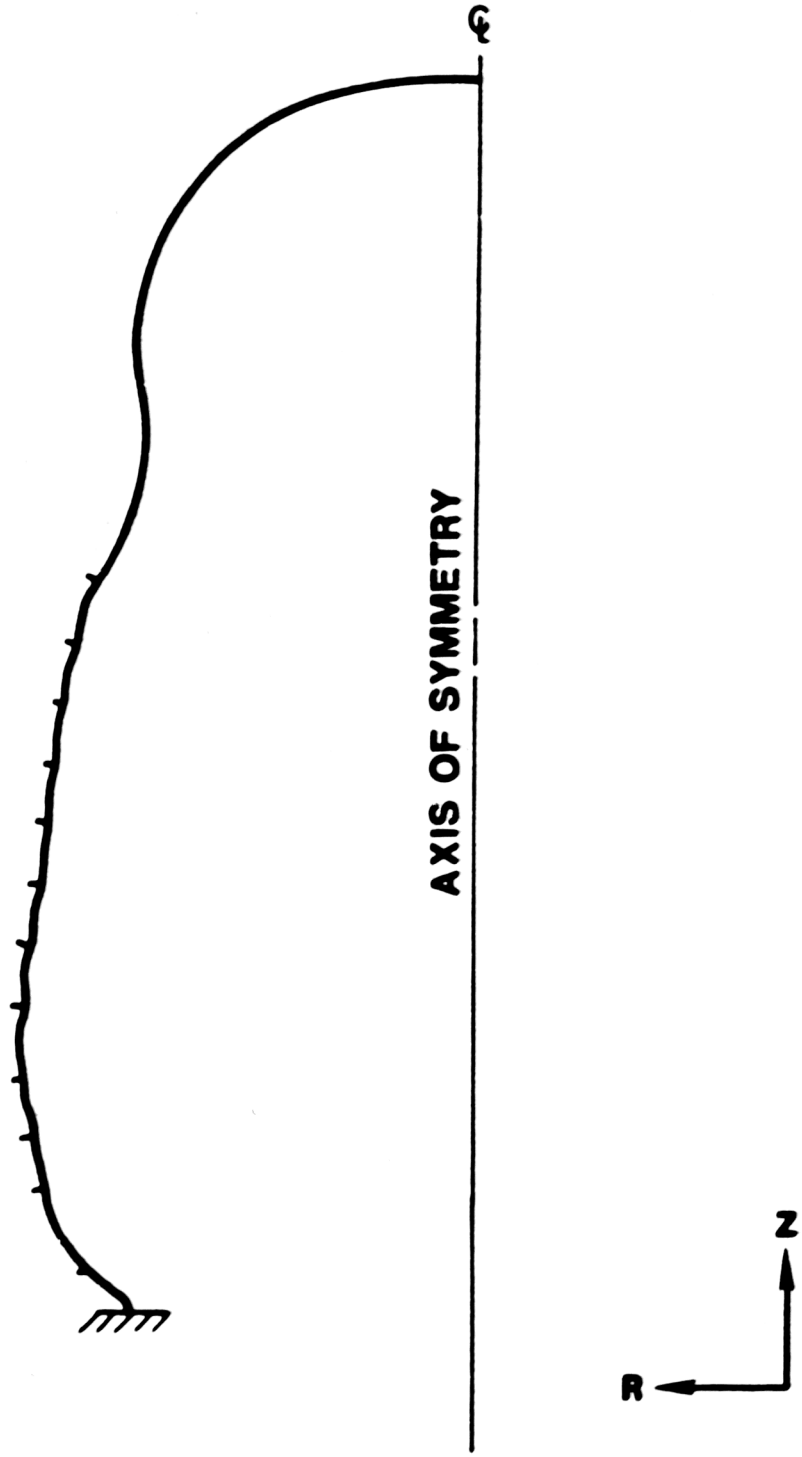


Figure 5

**Displaced Shape of the Watts Bar Containment at 160 psig**
(Displacement magnification of 10 x)

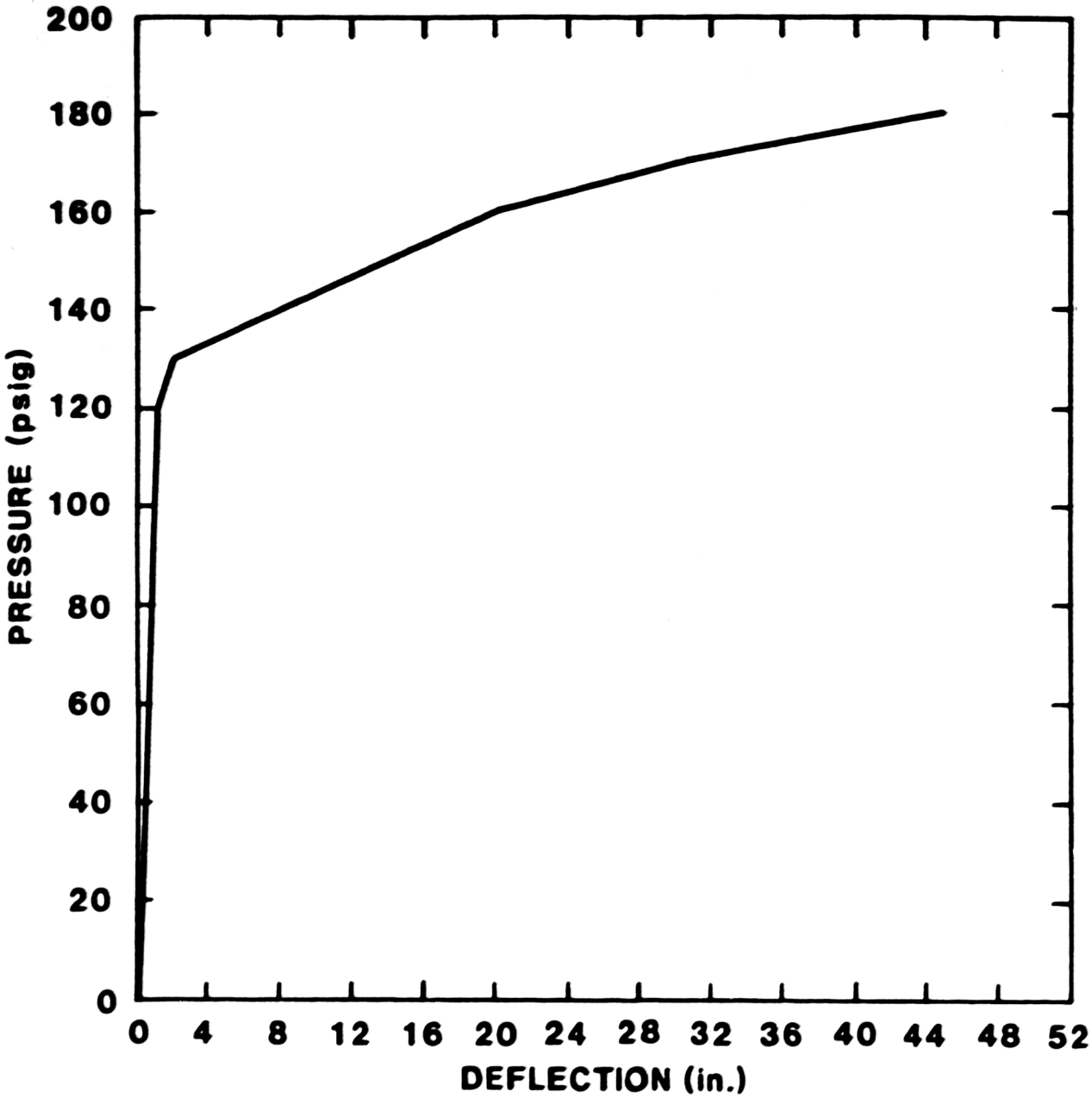


Figure 6

Radial Deflection at Mid Cylinder Height

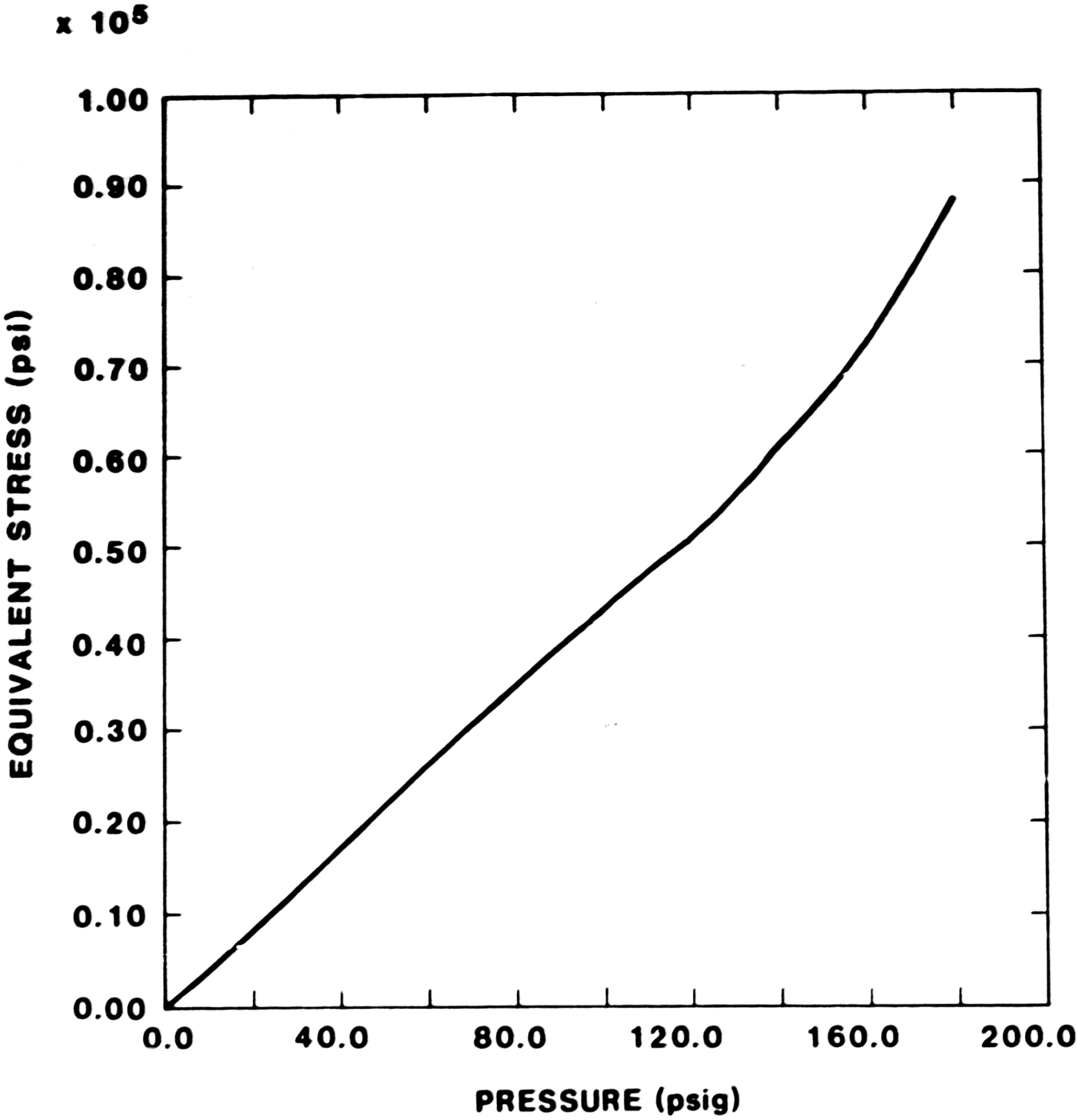


Figure 7

Equivalent Stress vs. Pressure at the Dome

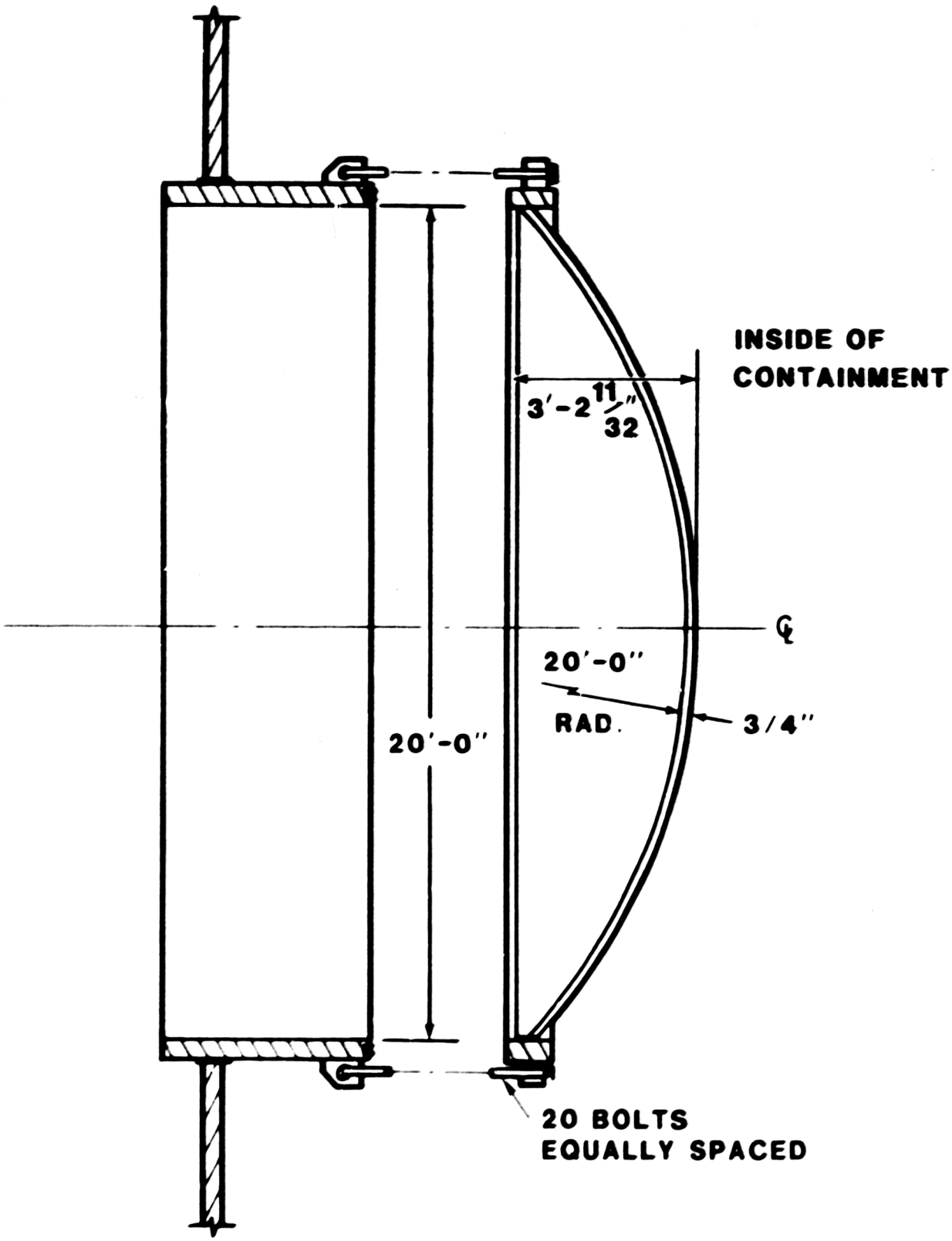


Figure 8

Equipment Hatch Section

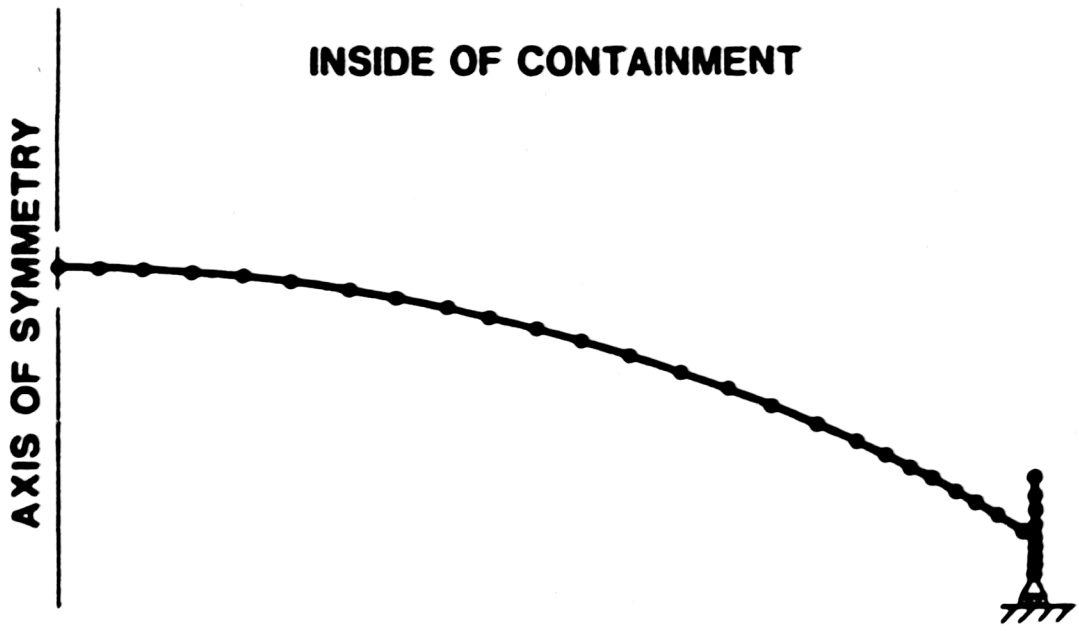


Figure 9

Axisymmetric Model of the Watts Bar Equipment Hatch Showing Element Subdivision

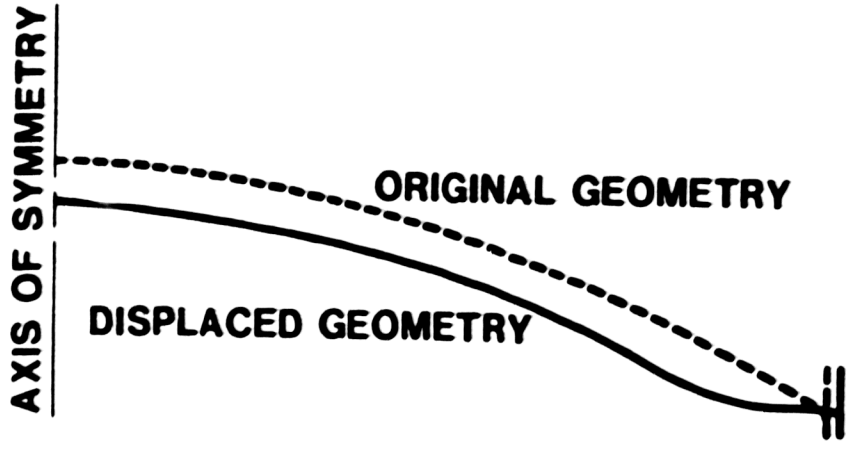


Figure 10

Displaced Shape Plot of Equipment Hatch at 137 psig
(Displacement magnification of 10 x)

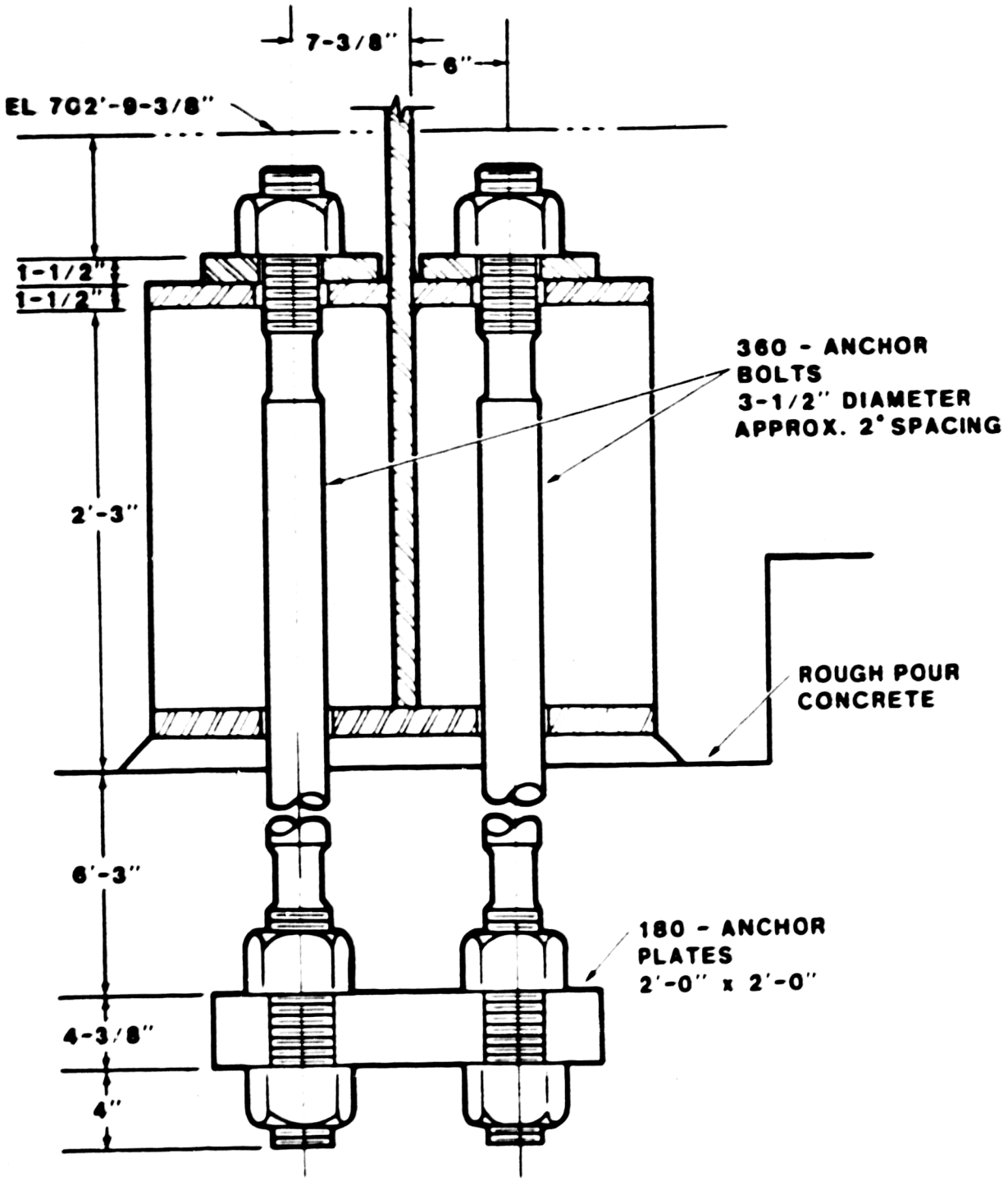


Figure 11

Watts Bar Containment Anchorage

## Personnel Lock Analysis

### Description of the Personnel Lock

The Watts Bar personnel lock, Figure 12, consists of a penetration sleeve with two 8-foot, 7-inch diameter cylinders. The ends are capped with 1/2-inch thick flat reinforced bulkheads having doors with double compression seals. The personnel locks are made from A516-GR70 steel.

### Finite Element Model

The computer code ABAQUS was used to perform the stress analysis of the bulkhead and door. The personnel lock sleeve was not included in the analysis. This nonlinear analysis utilized the large displacement, elastic-plastic options. Ninety-nine four noded, three dimensional shell elements and 18 beam elements were used. Because of the double symmetry, only one quarter of the bulkhead and door was modeled, Figure 13. The reinforcing stiffners were modeled with beam elements. Along the door bulkhead interface, displacement continuity was maintained but no moment transfer normal to the interface was allowed. This feature allowed the door and the bulkhead to be analyzed together and also assured the proper force transfer from the door to the bulkhead. The structure was loaded by applying pressure normal to the plane of the bulkhead.

The material properties for the analyses were constructed from Appendix A data in the same fashion as for both the containment shell analysis and the equipment hatch analyses.

The personnel lock sleeve was not included in the analysis because its inclusion would have greatly increased the complexity of the problem. The analysis was conducted using clamped boundary conditions on the outer bulkhead boundary. It is difficult to assess the conservative or nonconservative nature of this boundary condition short of actually performing an analysis that includes the sleeve, the containment-sleeve intersection and the loads transmitted from the containment to the sleeve. Such an analysis would require a significant analytical effort. Nonetheless, it was felt that the clamped boundary condition used for this analysis would provide a reasonable approximation to the actual boundary condition.

### Analysis Results

Figure 14 shows the displacement of the center of the door as a function of applied pressure; note that the stiffness of the structure increases after a displacement of approximately an inch has occurred. This effect is due to the increased

deformation allows the bulkhead to carry loads in a stiffer membrane mode as opposed to carrying loads primarily by bending as is the case at low pressures. A maximum displacement of 3.3 inches can be expected at the center of the door at a load of 150 psig. Figure 15 shows the displacement profile of the door and bulkhead along its horizontal centerline at various pressures.

Contour plots of von Mises equivalent stress at various pressures on the bulkhead and door mid plane are given in Figures 16 - 18. In these figures, the areas shown above 50 ksi equivalent stress have yielded. Initial outer fiber yielding along the outer boundary of the bulkhead occurs at a pressure of approximately 24 psig. This low yield pressure is most likely due to modeling the bulkhead boundary as a clamped end condition which would create artifically high stresses in that region when compared to the more flexible actual boundary condition of the bulkhead plate connected to the cylindrical sleeve. At a pressure of 64 psig, the bulkhead and door assembly act essentially as membrane structures and the midplane of the bulkhead material has begun to yield along the outer bulkhead boundary.

In regard to failure of the bulkhead and door, none of the contours in Figure 17 at 150 psig shows stresses even approaching the 74 ksi equivalent stress required for material failure. From this result it was deduced that the personnel lock bulkhead-door system has a structrual pressure capacity above 150 psig.

The analysis of the bulkhead and door system attempted to find when a structural collapse of the system would occur. There was no attempt made to estimate when possible leakage around the seals would occur.

## Summary of Watts Bar Results

A summary of the analysis results is given in Table 2. These results indicate that a realistic range for the ultimate capacity of the Watts Bar containment structure would be between the general yielding of the containment cylinder and buckling of the equipment hatch door, 120 and 140 psig, respectively. Although general yielding of the shell cylinder does not in itself mean the loss of containment capacity, it does suggest that possible failures due to structural interactions related to excessive deformations are more probable. It is believed that the 120 psig pressure can be interpreted as a lower bound to the containment capacity while there is a high probability of loss of containment capacity at the 140 psig.

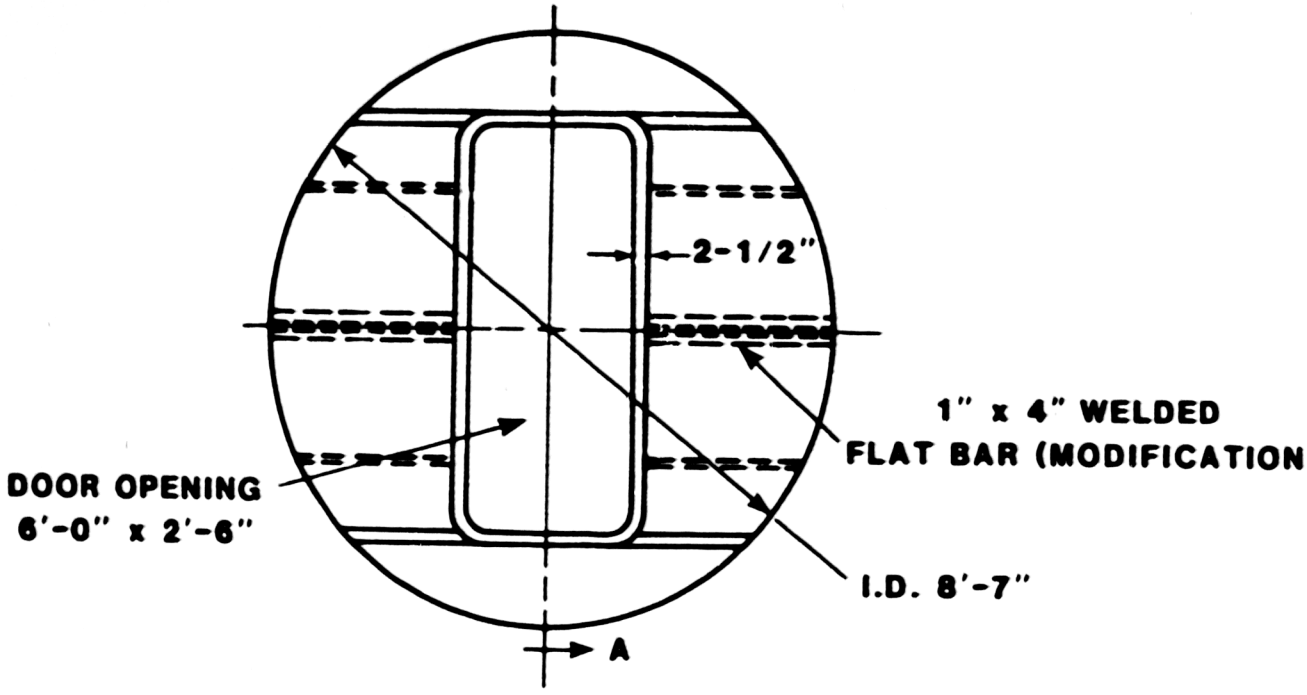


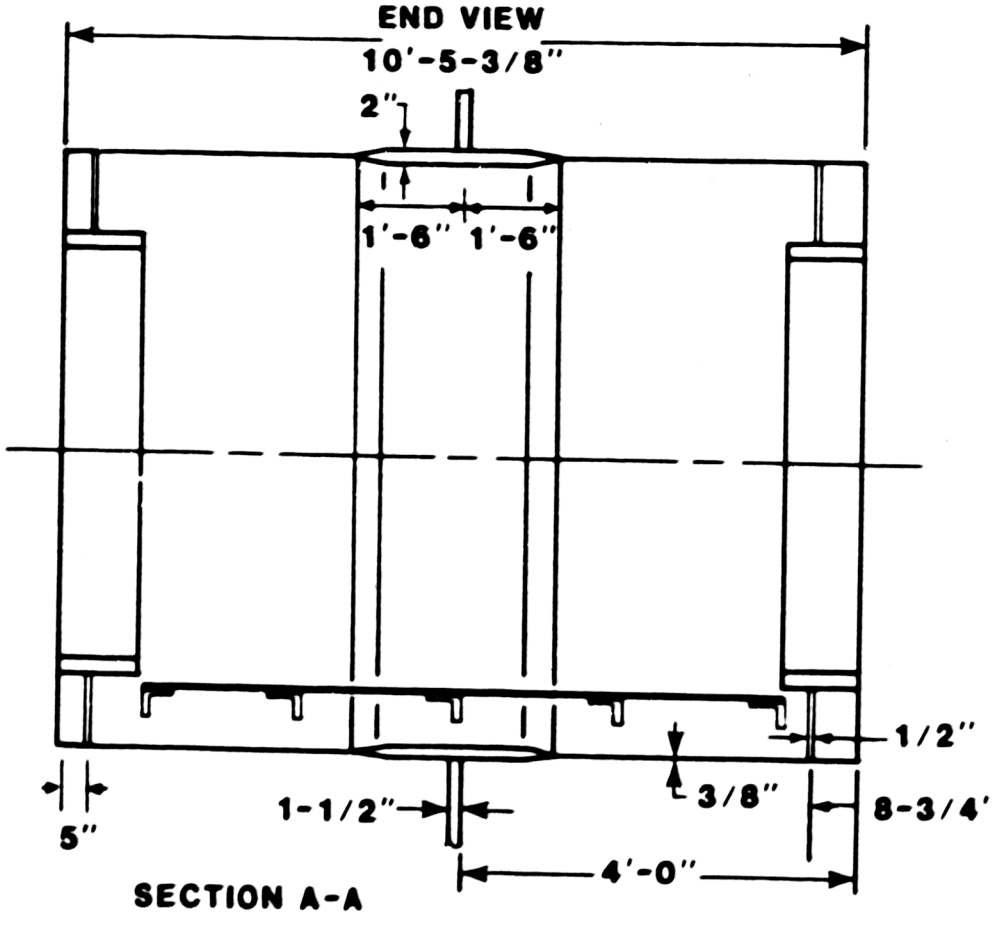


Figure 12

Watts Bar Personnel Lock

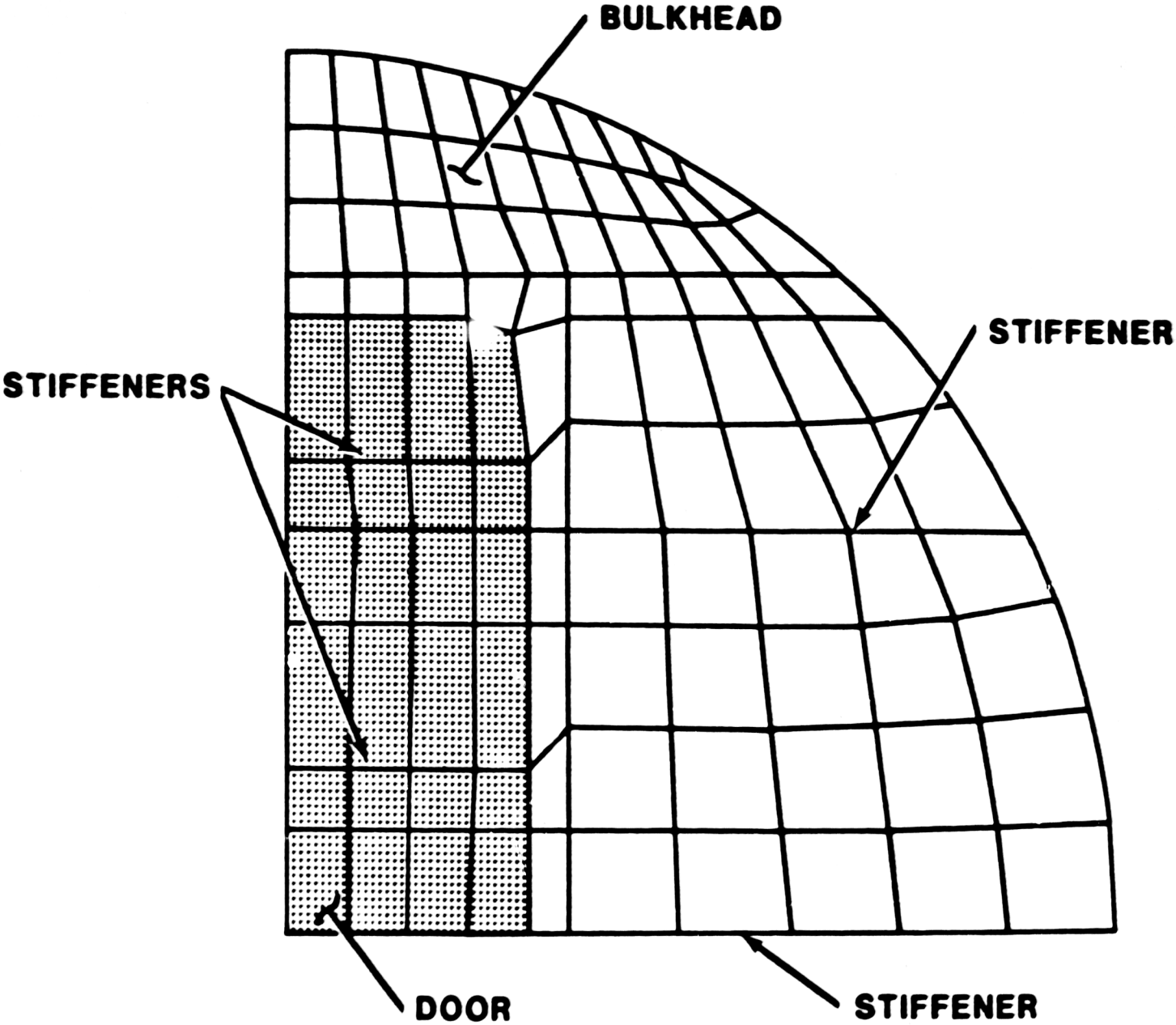


Figure 13

Watts Bar Personnel Lock Mesh

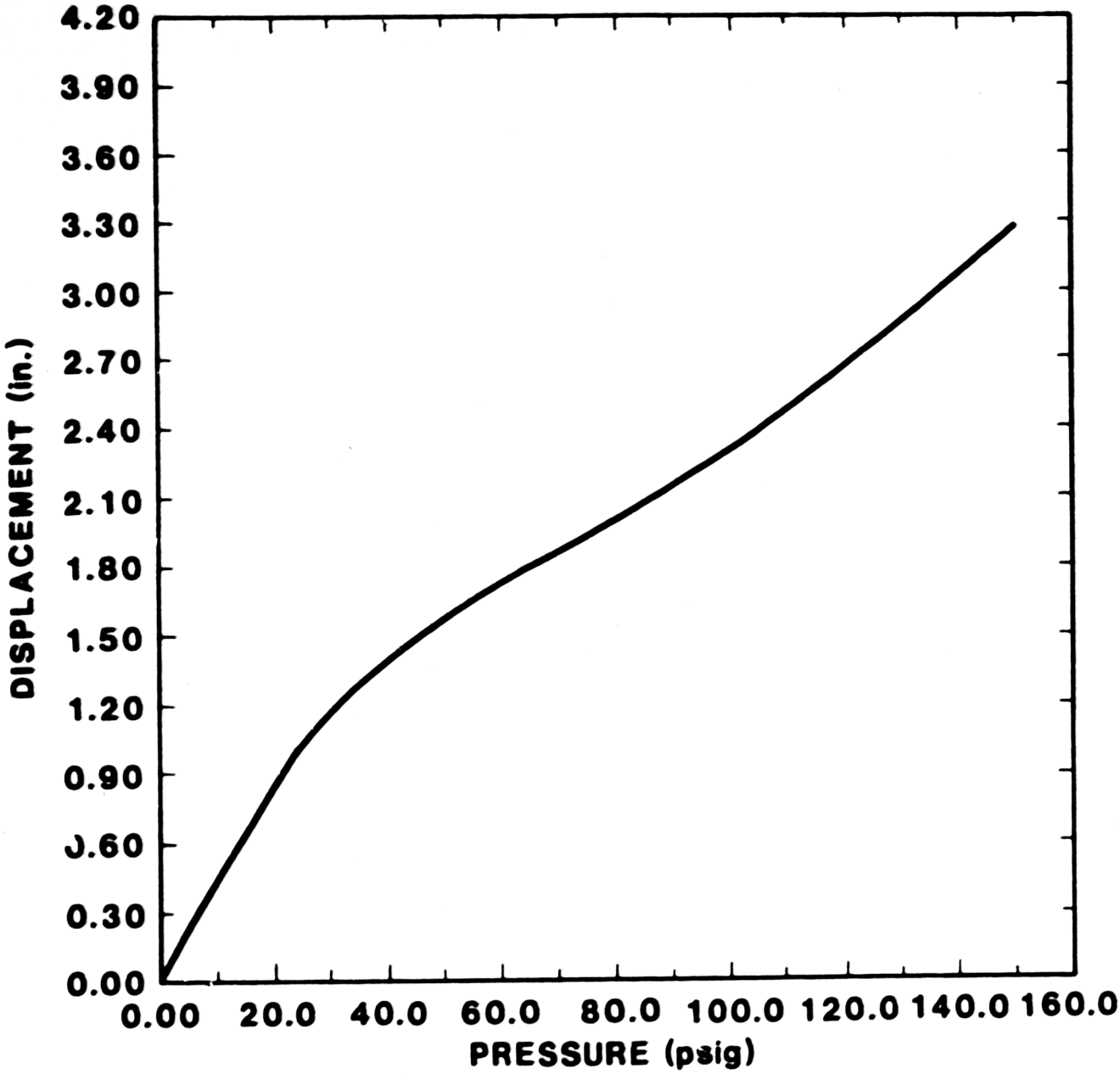


Figure 14

Displacement of the Center of the Personnel Lock Door as a Function of Pressure

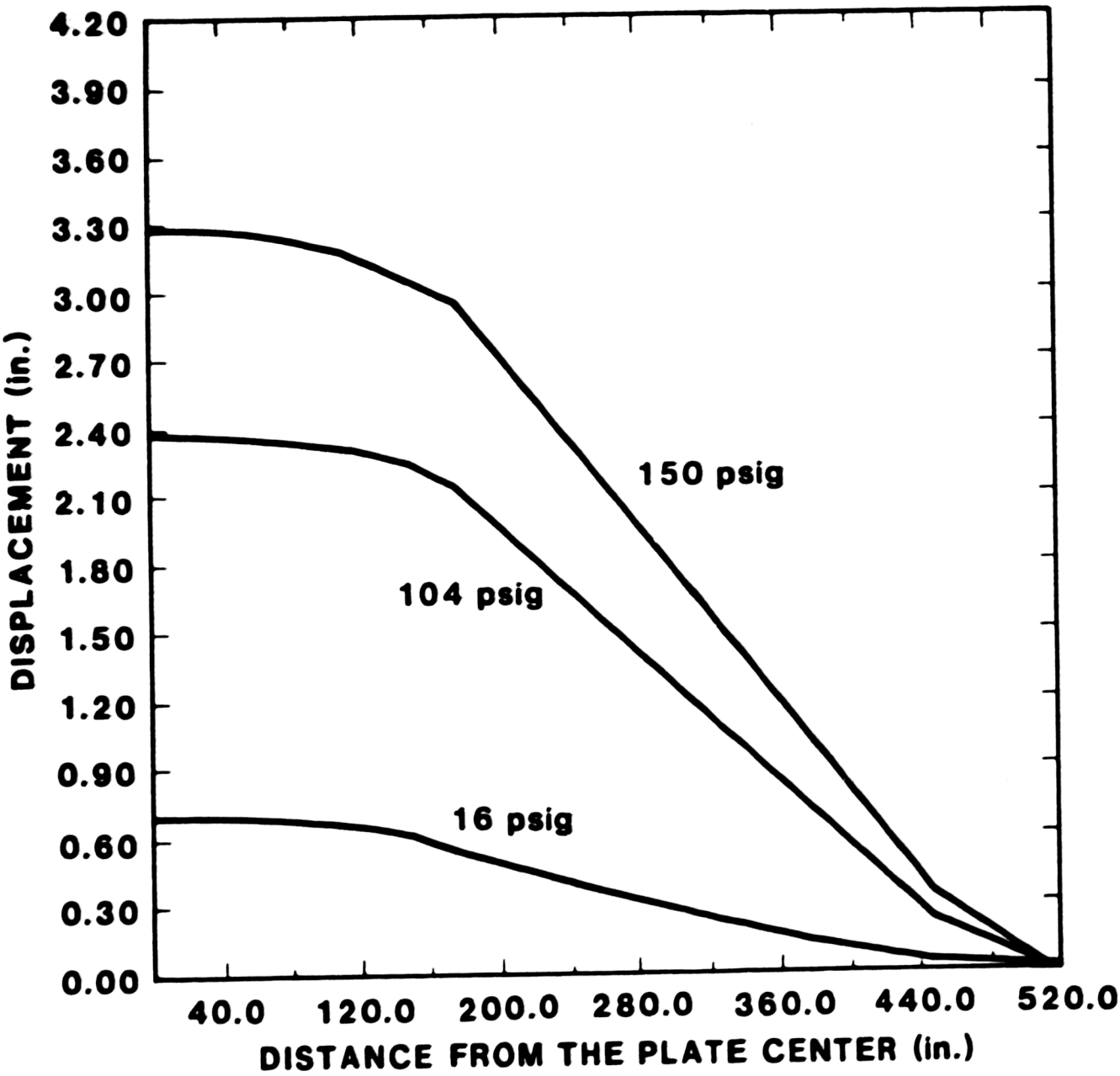


Figure 15

Displacement Profiles of the Door and Bulkhead
Along the Horizontal Axis of Symmetry

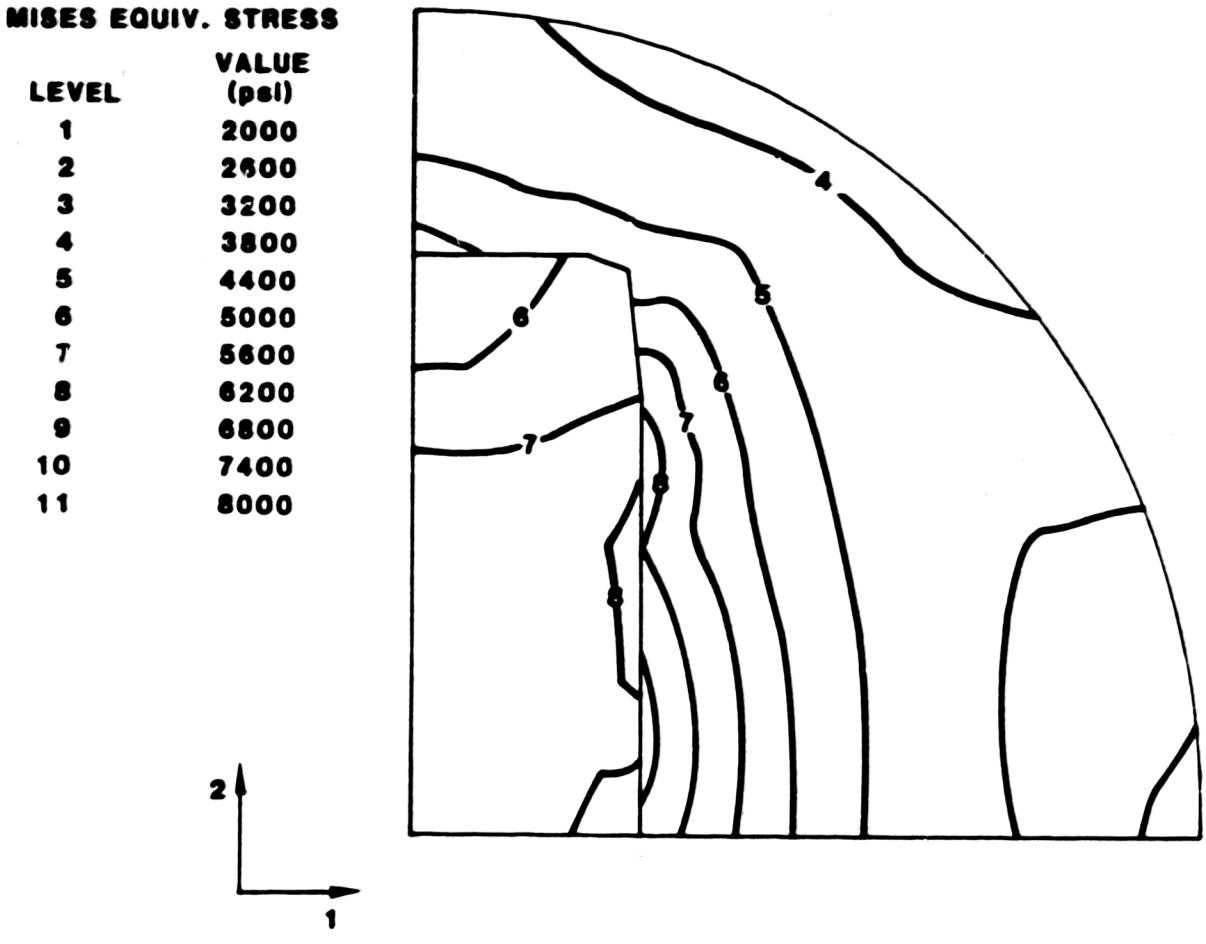


Figure 16

Contours of von Mises Equivalent Stress at 16 psig
at the Bulkhead mid Surface

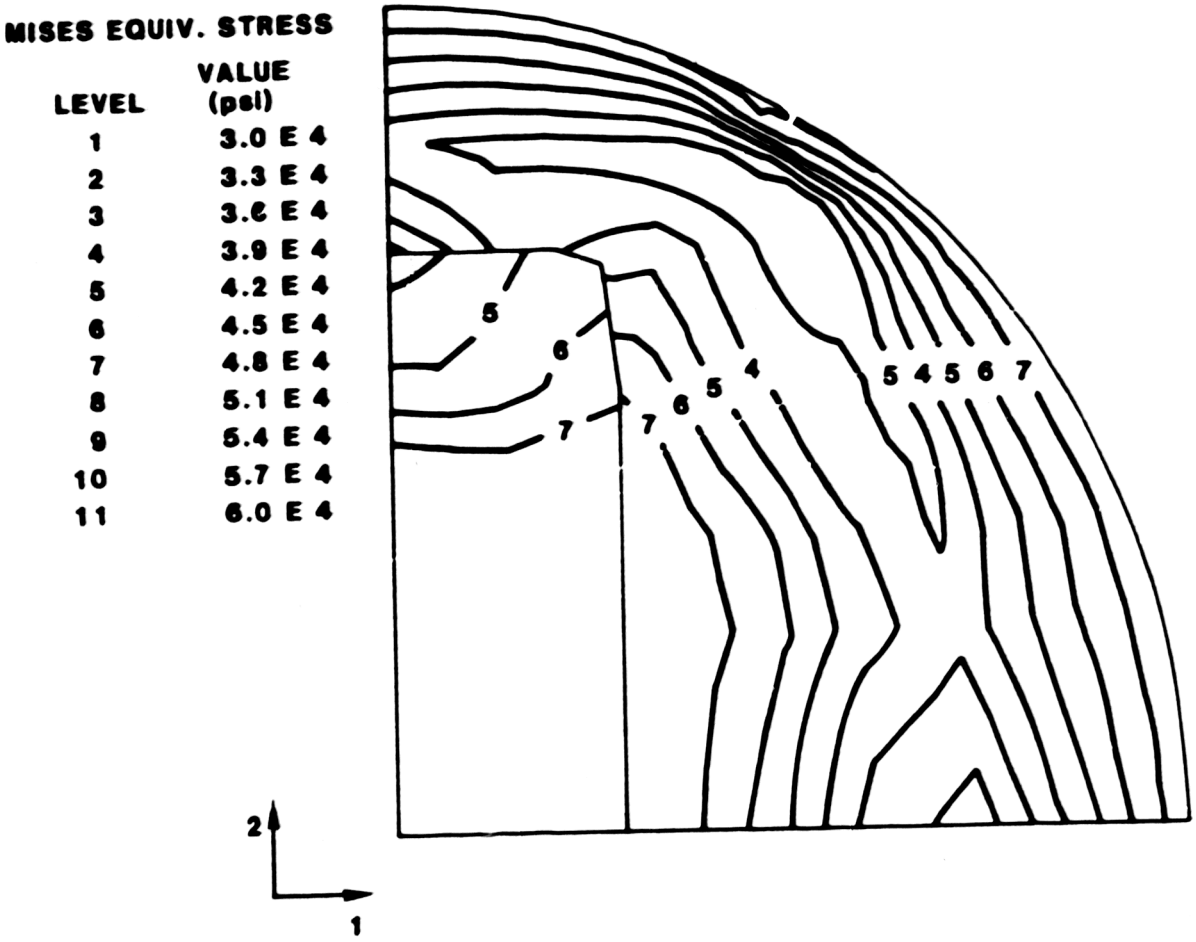


Figure 17

Contours of von Mises Equivalent Stress at 104 psig
at the Bulkhead mid Surface

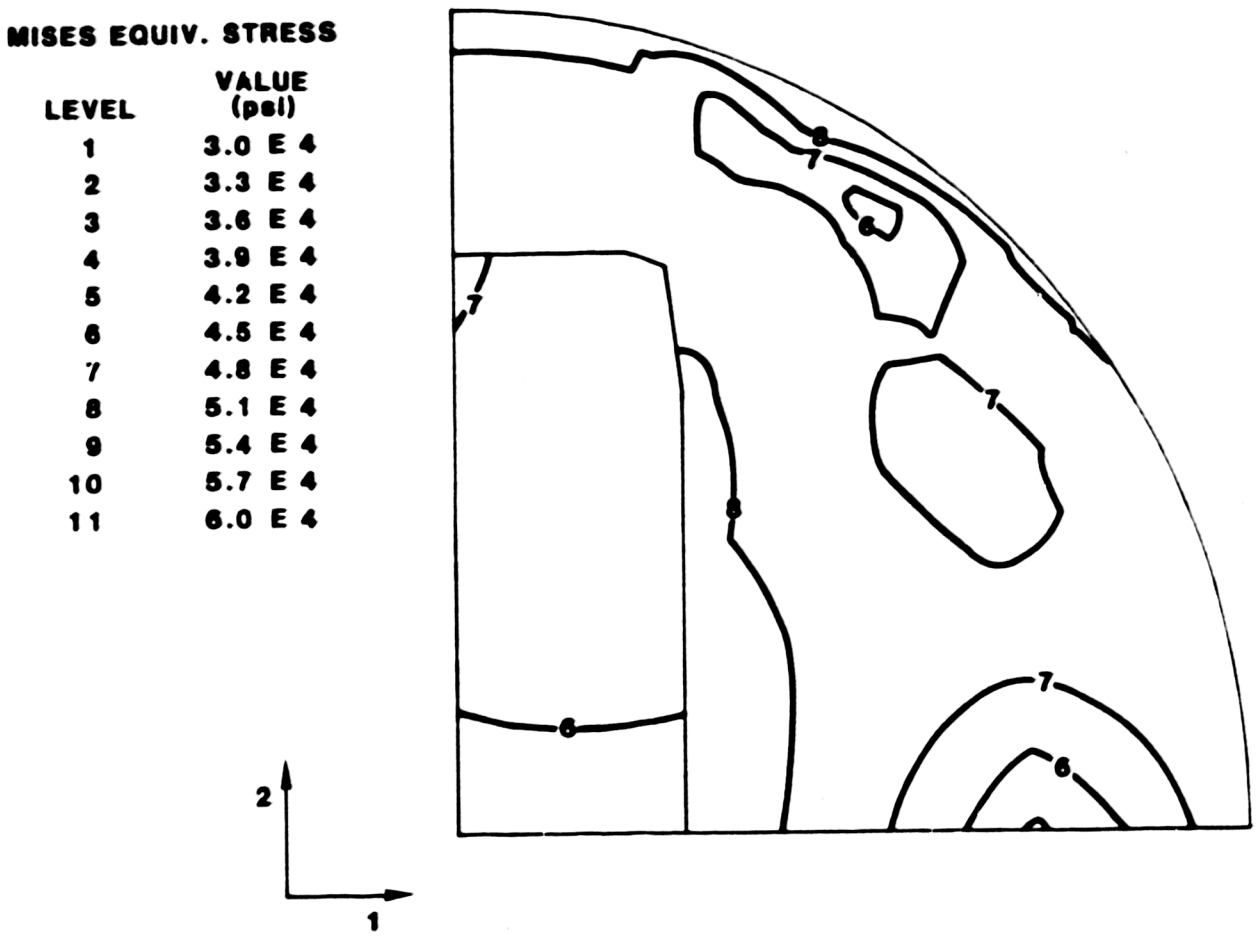


Figure 18

Contours of von Mises Equivalent Stress at 150 psig
at the Bulkhead mid Surface

Table 2

Summary of Results

| Component | Ultimate Capacity(psig) | Location or Mode of Failure |
|---|---|---|
| Containment Shell | 120/175 | General shell yielding/Dome failure |
| Equipment Hatch | 137 | Buckling |
| Anchorage System | 172 | Yielding of the Tie-Down Bolts |
| Personnel Lock | >150 | |

## MAINE YANKEE CONTAINMENT ANALYSIS

The Maine Yankee containment building is a reinforced concrete structure with a ductile steel liner. A structural analysis using static internal pressurization was performed with a modified version of the finite element code ADINA [6,7]. The material models in ADINA are capable of dealing with concrete cracking and crushing, and reinforcement and liner yielding. Unfortunately, as-built material properties were not available so the minimum specified properties were used in the analyses.

### Containment Building Description

The Maine Yankee containment building consists of a steel reinforced-concrete structure with a steel liner, Figure 19. The design pressure for the structure is 55 psig. The vertical height of the cylindrical wall is 102'-0" from the face of the concrete mat and the dome has an inside radius of 67'-6", making the overall inside height of the containment 169'-6", not including the reactor pit. The vertical cylindrical wall is 4'-6" thick and the dome is 2'-6" thick. The containment floor is covered with a 2' thick layer of protective concrete. A vapor-tight barrier for the reactor containment is provided by the steel liner which covers the containment floor and inside cylindrical wall and dome. The steel liner thickness is 1/2" at the dome, 3/8" at the cylindrical walls and 1/4" at the containment floor. There are no diagonal reinforcing bars in the containment wall.

The concrete used in the containment has a nominal 3000 psi specified compressive strength. The reinforcing bars [8] were made from A 408 steel with a minimum yield stress of 50,000 psi and an ultimate tensile stress between 70,000 and 90,000 psi. The liner was constructed from A 516 Gr. 60 steel. A summary of these material properties is given in Table 3. Number 18 bars were used for major reinforcement. A summary of the major reinforcing for the dome and cylindrical wall is given in Table 4.

### Finite Element Model

The axisymmetric finite element model of the containment structure, Figure 20, consisted of three types of elements. The concrete material was modeled using 212 two-dimensional solid elements. The containment reinforcement was modeled using truss elements, i.e. the longitudinal reinforcement was represented by 126 three-noded truss elements and the hoop reinforcement was modeled using 208 one-node ring truss elements. The steel liner was modeled using 57 axisymmetric shell elements [7]. The protective layer of concrete on the containment floor was not modelled.

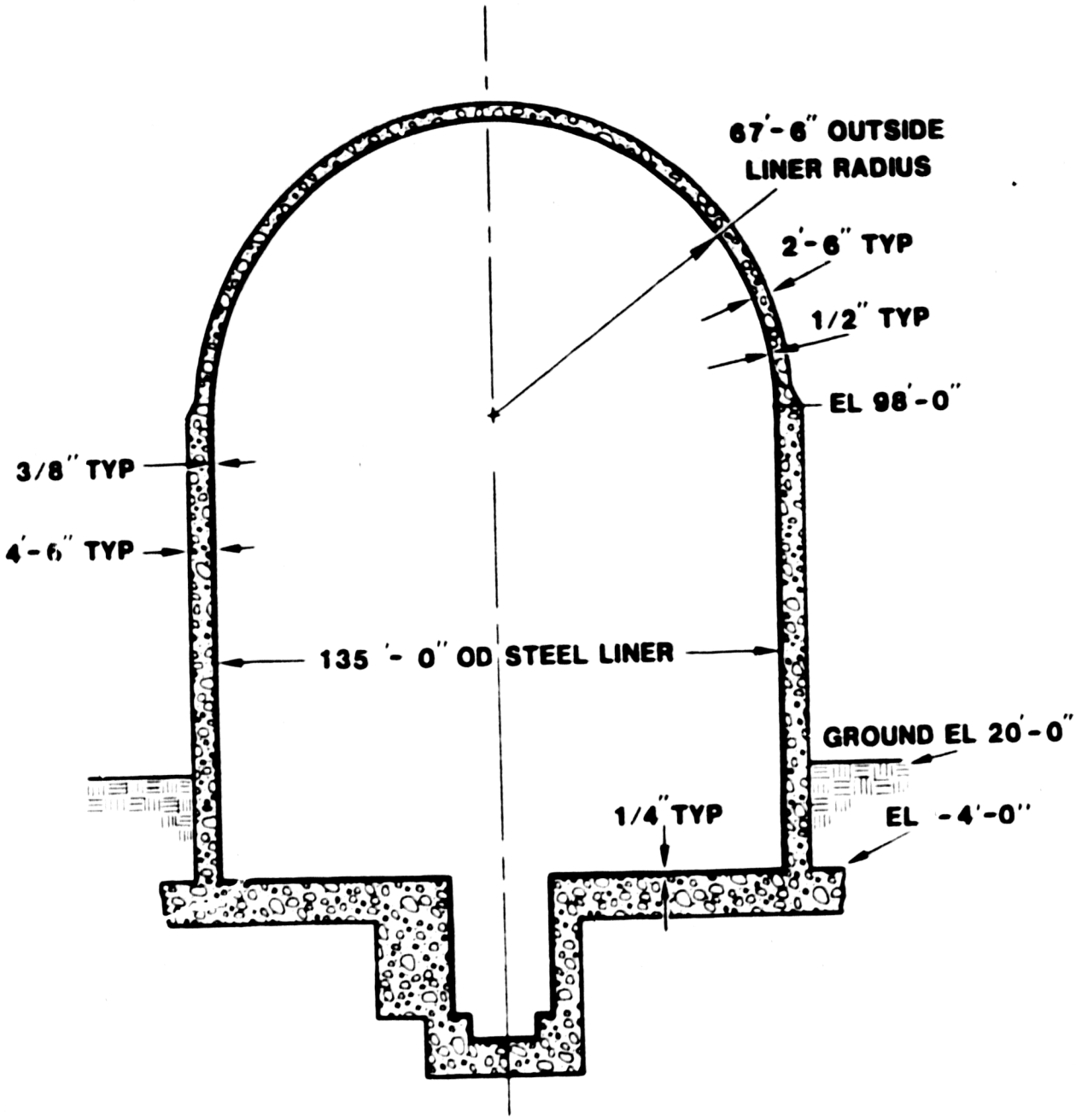


Figure 19

Maine Yankee Containment Structure

The two-dimensional solid elements used to represent the concrete were eight-node isoparametric elements using a 3 x 3 integration. The concrete material model in ADINA allows for cracking and crushing [6]. In this model a "crack plane" perpendicular to the maximum tensile principal stress is formed when the maximum tensile principal stress exceeds a designated value. When a crack plane forms, the tensile stiffness normal to the crack plane and the shear stiffness in the plane of the crack at that point are reduced. For this analysis the tensile stiffness and the shear stiffness were reduced to 0.0001 and 0.5 of their original valves, respectively. Concrete crushing occurs when a point established by the principal stresses fall outside of a predetermined failure envelope [9]. Some of the concrete material parameters used for this analysis are given in Table 5.

The longitudinal and hoop reinforcement in the containment is made from A408 steel. A yield stress of 50,000 psi and a plastic tangent modulus of 125,000 psi were used. These quantities are derived from the ASTM minimum values. The cross-sectional area of the longitudinal reinforcing elements was adjusted to account for the total number of reinforcing bars in the one radian section used for the axisymmetric analysis. The hoop reinforcements were placed on the interior and exterior wall nodes. The cross-sectional area of these elements were also adjusted to obtain the proper steel cross-sectional area.

The containment steel liner is constructed from A516 Gr. 60 steel. A yield stress of 32,000 psi and a plastic tangent modulus of 112,000 psi was used. These quantities are also derived from the ASTM minimum values.

Two axisymmetic analyses were conducted to investigate the importance of possible basemat uplift. The first used the boundary conditions shown in Figure 20 while the second analysis allowed for basemat uplift through the use of nonlinear truss elements along the foundation. These elements had high compressive stiffnesses and no tension stiffnesses. Any possible restraint of the cylinder side walls by earth was omitted.

## Static Pressurization

The initial solution strategy consisted of applying the gravitational loads, followed by the internal pressure in load increments of 0.5 psi. Unfortunately, at the onset of cracking in the hoop direction of the cylinder wall (cracking perpendicular to the hoop direction) the solution techniques available in ADINA were unable to converge to a solution. The program allows the user to specify a load step using the

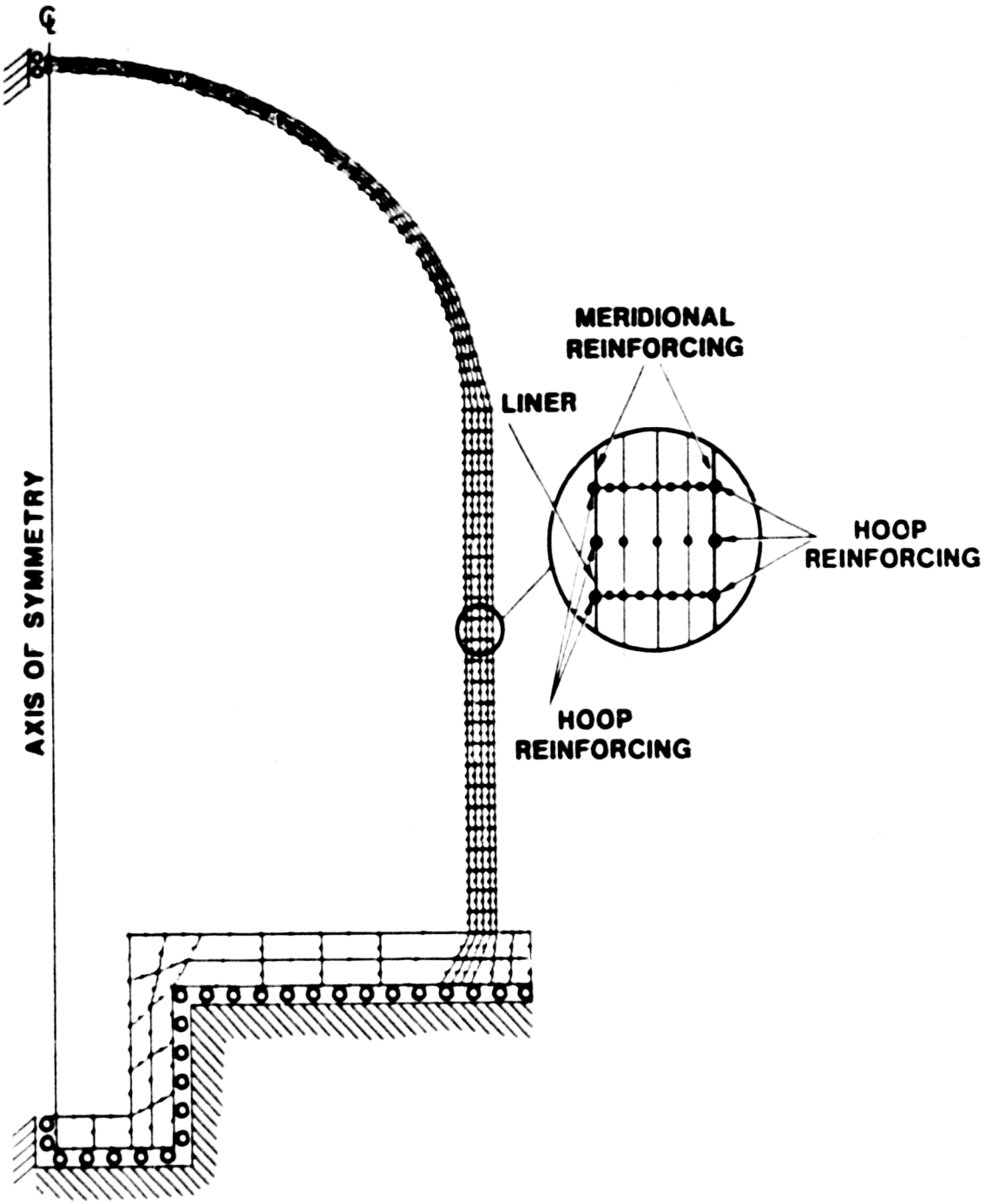


Figure 20

Axisymmetric Finite Element Model of Maine Yankee

Table 3

Summary of the Specified Maine Yankee Material Properties

| | |
|---|---|
| **Concrete** | |
| Minimum 28-day compressive strength | 3,000 psi |
| Maximum size of aggregate | 3/4" |
| **Reinforcing Bars** | |
| Steel type | A 408 |
| Minimum yield stress | 50,000 psi |
| Minimum elongation in 2" | 16% |
| Tensile ultimate stress | 70,000 to 90,000 psi |
| **Liner** | |
| Steel type | A 516 Gr. 60 |
| Minimum yield stress | 32,000 psi |
| Minimum elongation in 2" | 25% |
| Tensile ultimate stress | 60,000 to 80,000 psi |

Table 4

Summary of Major Dome and Cylindrical Wall Reinforcing

| Area | Direction of Reinforcing | Bar Size | No. of Layers | Spacing | No. of Bars/Layer |
|---|---|---|---|---|---|
| Dome R* < 11'6" | Radial | 18 | 2 | | 108 |
| Dome 11'6" < R* ≤ 25'9" | Radial | 18 | 2 | | 216 |
| Dome 25'9" < R* ≤ 54'9" | Radial | 18 | 2 | | 432 |
| Dome 54'9" < R* ≤ 67'6" | Radial | 18 | 2 | | 618 |
| Dome | Hoop | 18 | 2 | 9.5" o.c. | |
| Cylindrical wall El. -4' to 0.14' | Vertical | 18 | 3 | 12" o.c. | |
| Cylindrical wall El. 0.14' to 45' | Vertical | 18 | 7<br>2 | 5 @ 24" o.c.<br>@ 12" o.c. | |
| Cylindrical wall El. 45' to 98' | Vertical | 18 | 5<br>2 | 3 @ 24" o.c.<br>@ 12" o.c. | |
| Cylindrical wall | Hoop | 18 | 5 | 12" o.c. | |

* R denotes radial position from the axisymmetric centerline of the containment.

Table 5

Concrete Material Properties

| | |
|---|---|
| Initial tangent modulus | $3.14 \times 10^6$ psi |
| Poisson's ratio | 0.20 |
| Uniaxial tensile strength | 356.0 psi |
| Maximum uniaxial compressive stress | -3000 psi |
| Uniaxial compressive strain at maximum compressive stress | -.0018 |
| Ultimate uniaxial compressive stress | -2000 psi |
| Uniaxial compressive strain at ultimate compressive stress | -0.004 |

An alternate estimate of the containment ultimate capacity of 117 psig was obtained by computing the pressure associated with general yielding of the hoop reinforcing and liner at the cylinder wall. This hand calculation is in very good agreement with the above analysis result of 118 psig.

In the second analysis, which allowed for basemat uplift, the initial cracking again occurred at 31 psig with cracks in approximately the same areas as the first case. By 57 psig, though, both hoop and in-plane cracking had progressed through almost the entire horizontal portion of the basemat. First liner yielding again occurred at 73 psig. As the pressure was increased, the liner yielding progressed, and at 96 psig all of the liner from approximately 20 feet above the basemat to the apex of the dome had yielded. At 96 psig a numerical instability was encountered because the equations of equilibrium in the basemat cylinder wall intersection region were ill-conditioned. At this point the concrete in this region was so severely damaged that the numerical analysis could not be continued.

Whether a true structural failure corresponds to the numerical instability is questionable and probably would depend on the details, e. g., whether the damage to the concrete was severe enough to not allow the reinforcing bars to develop their full capacities. This question is apparently not addressable with the current state of the art of concrete analysis. The 96 psig pressure represents a lower bound pressure capability for the Maine Yankee concrete structure. The midcylinder height radial displacement for this case is also shown in Figure 21. The differences in the uplift and no uplift plots are apparent only after 70 psig. The basemat uplift of approximately 10 inches at 90 psig is shown in Figure 22.

## Maine Yankee Summary

The finite element analyses of the Maine Yankee containment building subjected to static internal pressurization indicated that initial hoop cracking of the containment wall would occur at 31 psig followed by liner yielding at 73 psig. If basemat uplift is accounted for, severe concrete damage in the basemat cylinder wall intersection region will occur. In the present numerical analysis, this damage was severe enough to cause a termination of the analysis at 96 psig. When the basemat uplift was not allowed, the analysis was continued above 118 psig at which pressure general yielding of the cylindrical wall reinforcing bars occurred. The 96 psig internal pressure value represents a lower bound estimate for the ultimate structural capacity of the concrete containment.

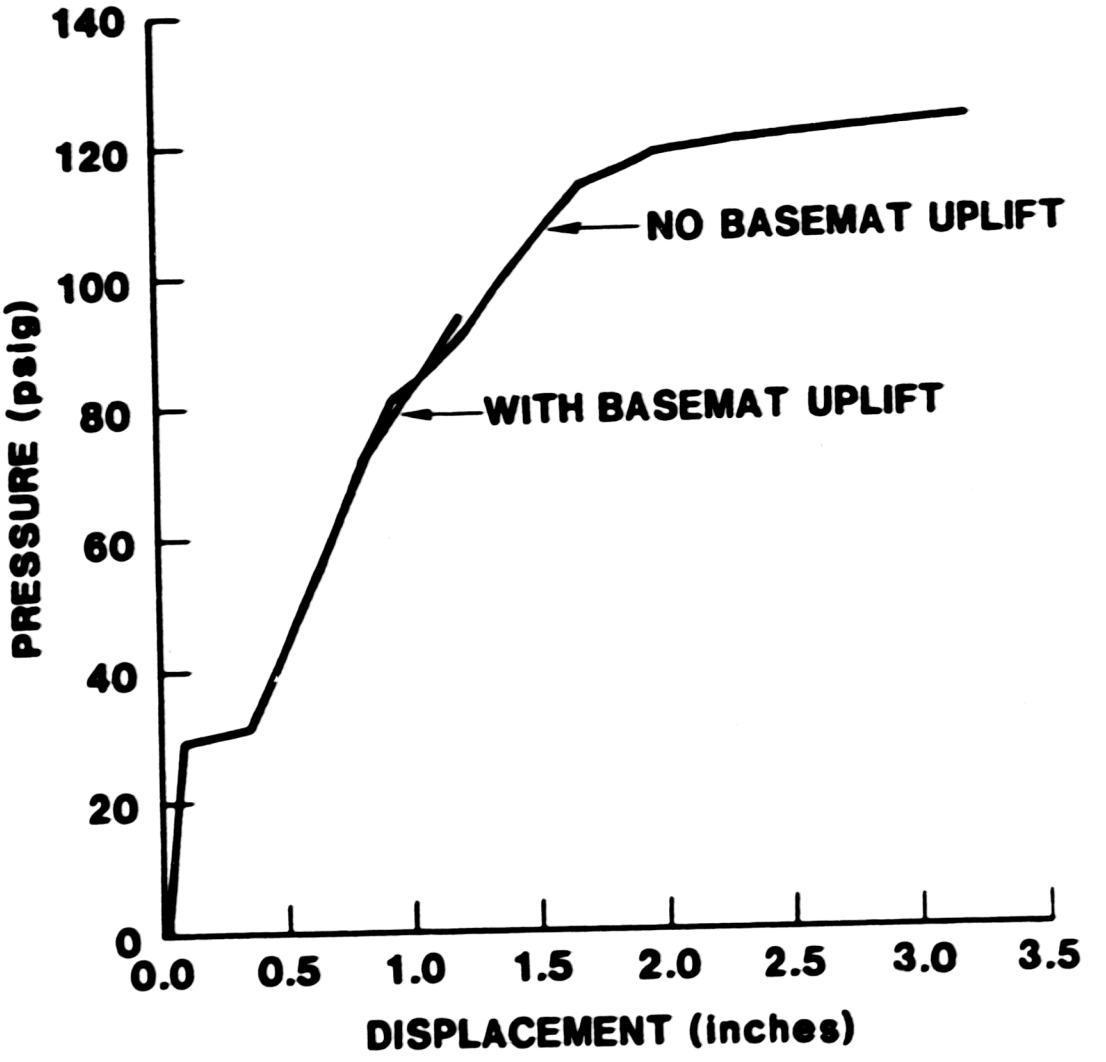


Figure 21

Radial Displacement of the Cylinder Wall at Midheight

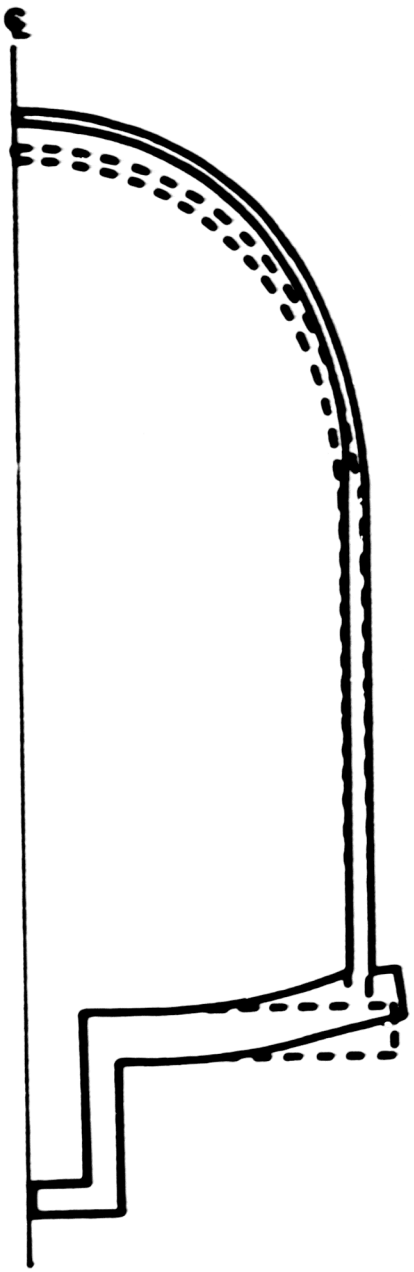

Figure 22

Displaced Shape of the Maine Yankee
Containment With Basemat Uplift at 90 psig.
(Displacement magnification of 10x)

Given that the analyses reported herein were performed using minimum allowable material properties and not as-built properties, the ultimate capacity estimates of the concrete containment are probably conservative. Other potential failure modes, such as penetration failures, were not addressed.

## BELLEFONTE CONTAINMENT ANALYSIS

### Containment Building Description

The Bellefonte primary containment, Figure 23, is a prestressed concrete structure consisting of a 1/4 inch thick steel liner, steel reinforcement, and prestressing tendons [11]. A unique feature of the Bellefonte containment is the rock anchor system that ties the cylindrical walls to the rock foundation. This feature eliminates the typical basemat found in most concrete containments.

The containment cylindrical wall has an inside diameter of 135 feet, a height from the base slab to spring line of 227 feet, and is 3 feet 6 inches thick. There are four equally spaced exterior concrete buttresses around the cylindrical wall. Each horizontal tendon is anchored at buttresses located 180 degrees apart. The vertical tendons are fastened to the prestressed rock tendons by coupling devices located in the tendon access gallery.

The elliptical dome roof is 3 feet thick and is prestressed by three groups of tendons.

The primary containment structure is enclosed within a free standing, reinforced concrete secondary containment. The secondary containment provides missile protection for equipment within the 10 foot annulus area.

### Finite Element Modeling of the Containment Shell

An axisymmetric finite element analysis of the containment shell was performed. The finite element model, Figure 24, consisted of 237 axisymmetric continuum elements and 57 three noded axisymmetric shell elements. Eight noded isoparametric continuum elements were used to represent the concrete. The reinforcing bars and prestressing tendons were embedded in the elements. The shell elements were used to model the containment's steel liner. The finite element code ABAQUS[2], version 4.5.71, was used to perform the analysis.

Of course, the Bellefonte containment is not truly axisymmetric. The variation of reinforcing and tendon patterns around the major penetrations were ignored. The extra steel reinforcing in these areas makes them less likely to fail than the general shell regions. The dome tendon arrangement is also not axisymmetric. In the finite element model, the dome tendon geometry was approximated with an axisymmetric representation.

The ABAQUS computer code uses the Chen and Chen constitutive theory for concrete [12]. The theory is basically a plasticity theory with a yield surface used to define the salient features of concrete. The implementation of this theory in the ABAQUS code allows the concrete to crush and crack. If crushing occurs, the concrete loses all of its strength instantaneously. If cracking occurs, cracks will form in a plane orthogonal to the largest tensile strain direction and the tensile strength of the material is lost. An unloading portion of the stress-strain curve is used to control how quickly the strength of the concrete is lost.

The Bellefonte liner is constructed from A516 GR 70 steel while the reinforcing bars were constructed from A615 GR 60 steel. Each prestressing tendon consists of 170- 1/4 in. diameter wires. The finite element analysis utilized average actual material properties. These properties were obtained from either mill test reports or Tennessee Valley Authority data [13] of the Bellefonte containment material. A summary of the average properties is given in Table 6, and a listing of the mill tests report data is given in Appendix B.

## Static Pressurization of the Containment

The analysis was conducted by first applying the prestress and then the internal pressure in the structure. The prestress was applied incrementally by specifying a series of temperature changes in the structure with the coefficients of thermal expansion of all the containment materials, except that of the tendons, set to zero. This technique allowed the prestress to be applied gradually so that the nonlinear behavior of the concrete could be followed. Also, pronounced nonlinear behavior of the concrete at the top of the dome during prestressing necessitated using a linear constitutive representation for the concrete in the row of elements adjacent to the centerline.

After the prestress was applied, the internal pressure of the containment was increased in one psi increments until a clear indication of containment failure was reached. Because of the severe and abrupt nonlinear behavior of the concrete, smooth convergence to a satisfactory solution at a given load was not

always possible, even when using a full Newton technique. Therefore, the analysis was conducted by allowing the program to iterate no more than a fixed number of times at a given load step. If the residual forces reached acceptably low values during the iteration process, the analysis continued to the next load step. If the residual forces did not reach acceptable levels at the end of the maxium allowed number of iterations, the program was directed to go on to the next load step and continue the analysis even though convergence was not met. The residual forces are carried over to the next step, though. The initial attempts to conduct this analysis showed that smooth convergence could not be expected and that convergence may be very slow, making it impractical to apply conventional convergence criteria to this problem. For this analysis, a maximum of four iterations was allowed for pressures below 100 psi, and a maximum of three iterations was allowed for pressures above 100 psi. The change in the allowable number of iterations was based on the results of the previous runs that showed that the solution was not significantly improved with four rather than three iterations.

The results of the analysis show that after the prestress was applied, the top of the dome was lowered by 1.2 inches and the cylinder wall at midheight had come in radially by 0.17 inches, Figure 25. The magnified deformed shape of the inside surface of the containment after the prestress had been applied is shown in Figure 26.

Little nonlinear behavior was exhibited below an internal pressure of 110 psig. At that pressure cracking began to occur in the dome concrete. At 120 psig, yielding of the liner in the dome had begun and cracking of the dome concrete increased. By 130 psig, yielding of the dome tendons had occurred accompanied with gross cracking of the concrete adjacent to the yielded tendon areas. The structural integrity of the dome is questionable at this pressure level because of the loss of stiffness in the tendons and the severe damage to the concrete. The magnified displaced shape of the inner surface of the containment at 100 and 130 psig internal pressure is also shown in Figure 26. There is, though, an added degree of uncertainty associated with this failure mode since the nonaxisymmetric dome tendon placement was approximated as axisymmetric for the analysis. It is difficult to determine the effect of this representation short of performing a three dimensional analysis.

Little damage to the containment in areas other than the dome was noted at 120 psig and only the dome tendons were yielded at 130 psig. A hand calculation performed to estimate the pressure associated with cylinder wall general yielding gave a pressure of 139 psig.

## Equipment Hatch Analysis

The Bellefonte equipment hatch is constructed from A516-Gr 70 steel. The disk portion of the hatch consits of a 1-inch thick spherical cap of 180 in inside radius. This cap is attached to a 4.5" by 7" outer steel ring. The steel ring is approximately 22 feet in diameter.

A structural analysis of the Bellefonte equipment hatch was performed using the ABAQUS Version 4-4. The average acutal material properties were used for the analyses. The finite element model, Figure 27, consisted of 81 nodes and 40 elements. The elements were three noded axisymmetric shells. The boundary conditions were identical to that used for the Watts Bar equipment analysis, i.e., symmetry conditions at the dome apex and only radial displacement allowed at the base of the ring. The finite element results indicated that the buckling capability of the hatch is above 169 psig. This pressure is significantly above the 139 psig pressure that is expected to cause general yielding of the cylindrical walls of the containment.

## Bellefonte Summary

The finite element analysis of the Bellefonte containment building subjected to static internal pressurization indicated that the building will fail at an internal pressure between approximately 130 psig and 139 psig. The lower pressure is associated with dome tendon yielding and the upper pressure corresponds to cylinder wall yielding. The buckling capacity of the equipment hatch is expected to be greater than 160 psig. Failure of other containments components were not addressed.

**Table 6**

**Summary of the Bellefonte Containment Material Properties**

Concrete

| | | |
|---|---|---|
| Number of Samples | - | several hundred (exact number unknown) |
| Average Compressive Strength | - | 6.85 ksi |

Steel

| Component | # Samples | Yield Stress (ksi) | Ultimate Stress (ksi) | Elongation % |
|---|---|---|---|---|
| #11 rebar | 48 | 67.4(4.01) | 105.1(4.46) | 13.1(4.96) |
| #9 rebar | 16 | 69.9(3.69) | 108.2(6.92) | 12.2(3.20) |
| #8 rebar | 37 | 72.7(4.59) | 110.3(6.03) | 14.5(1.44) |
| #6 rebar | 26 | 67.8(4.04) | 107.1(7.03) | 13.3(2.03) |
| Liner | 85 | 45.8(2.75) | 64.3(2.21) | 26.5(2.05) |
| Tendons | 100 | 228.7(10.1) | 252.9(5.17) | ---------- |
| Equipment Hatch | 8 | 50.8(1.19) | 79.9(1.67) | 29.38(0.52) |
| Personnel Lock | 28 | 51.8(4.22) | 74.9(3.21) | 25.9(2.45) |

*The first number is the average value and the second is the standard deviation.

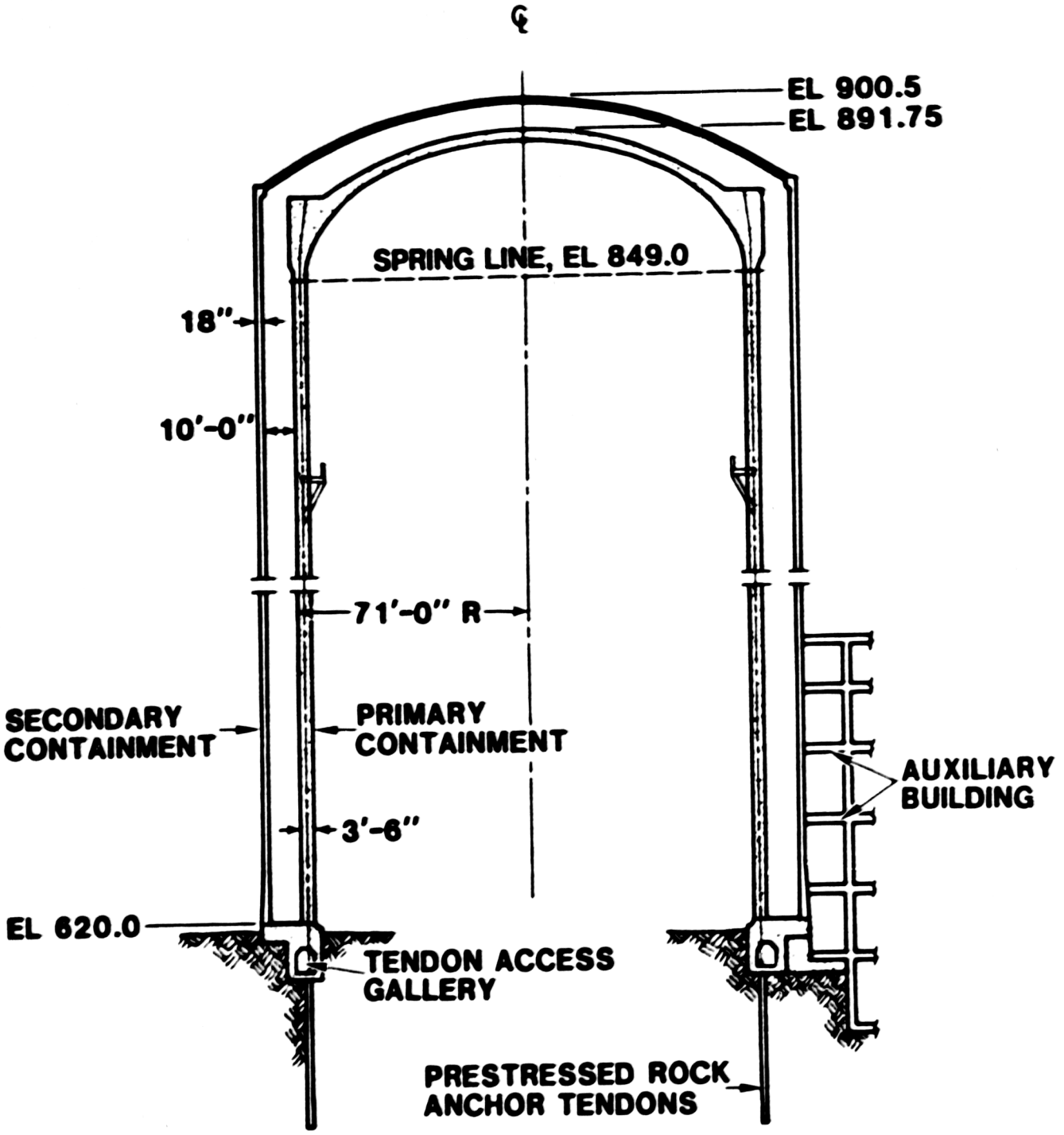


Figure 23

The Bellefonte Containment Structure

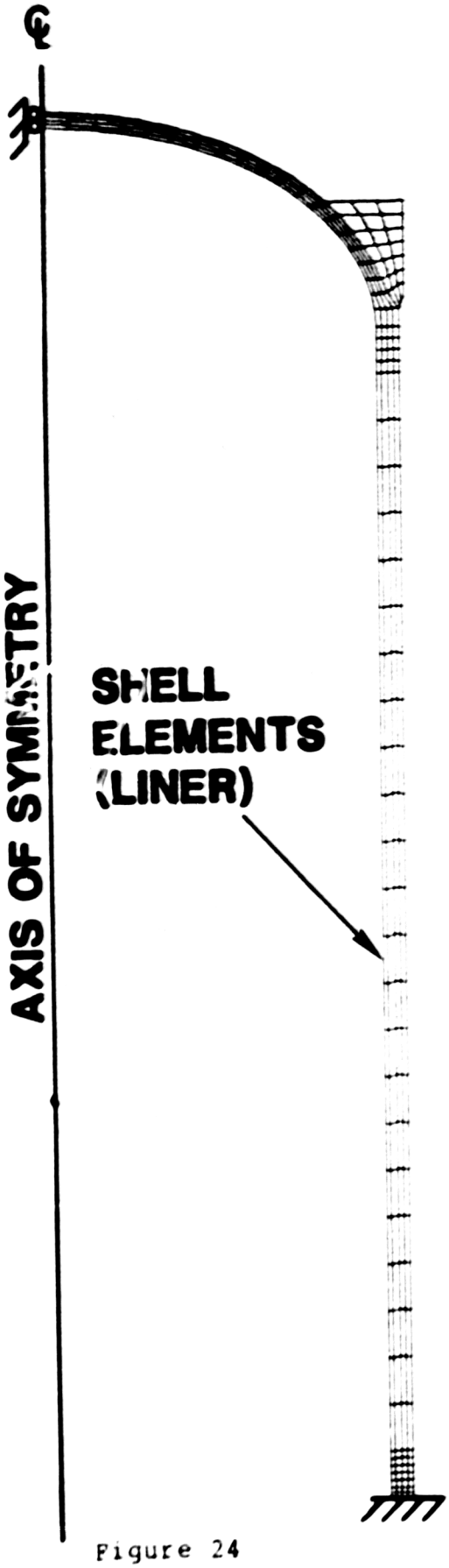


Figure 24

Axisymmetric Finite Element
Model of the Bellefonte Containment

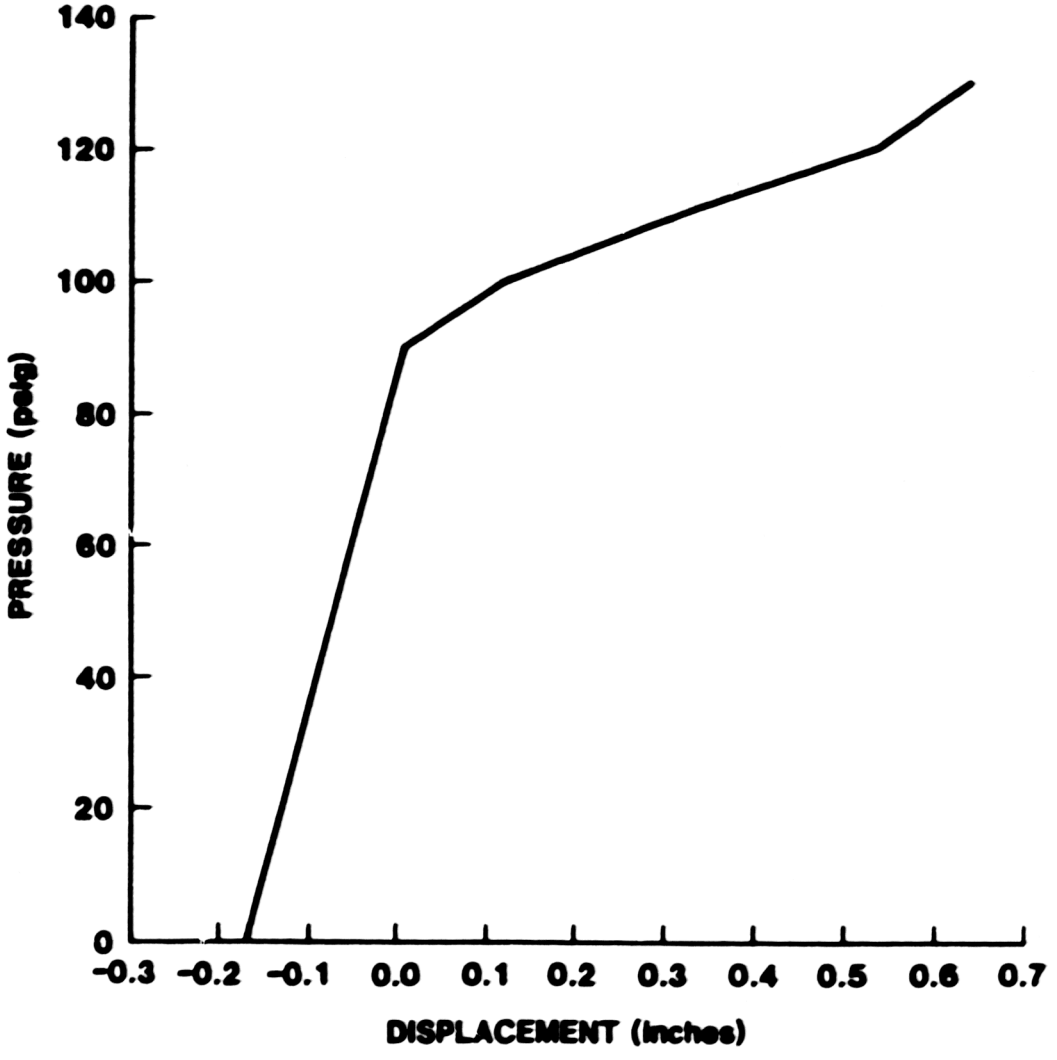


Figure 25

Displacement of the Bellefonte Containment at Mid Cylinder Height as a Function of Pressure

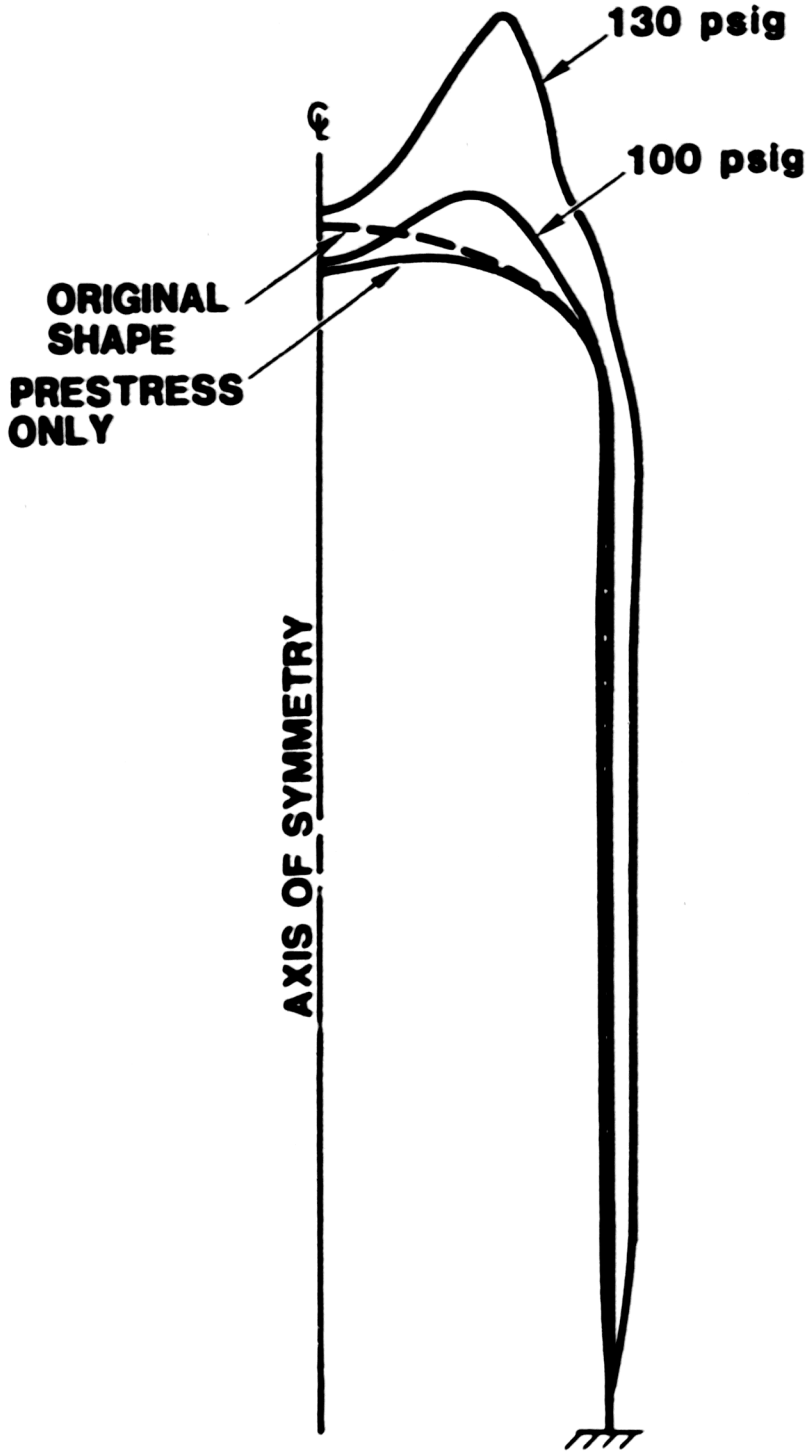


Figure 26

Displaced Shape of the Inner Surface of the Bellefonte Containment at Various Pressures (Displacement magnification of 100x)

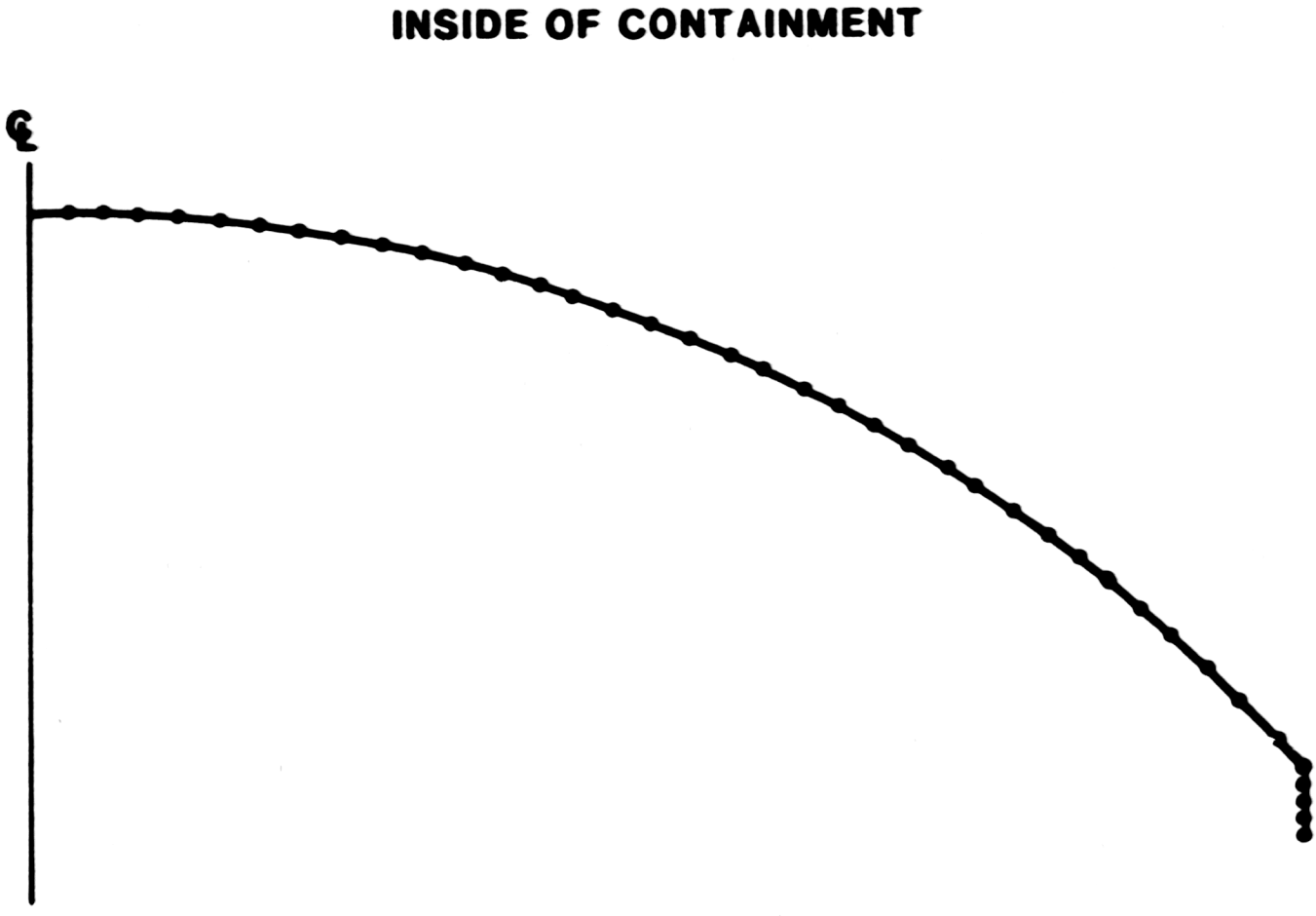


Figure 27

Finite Element Model of the
Bellefonte Equipment Hatch Showing Element Subdivisions

## References


1. MARC Analysis Research Corporation, MARC General Purpose Finite Element Program User Manual, Version J.1, , 1980.

2. Hibbitt, Karlsson and Sorensen, Inc., ABAQUS Users Manual, Version 4.5.71, July, 1982.

3. Cox, P.A.; Hokanson, J.C., Lindholm, U.S.; Nagy, A., Baker, W.E.; Dynamic Response, Impact and Materials Test Studies of Explosion Test Vessels, Final Report SwRI Project 02-4810, February 28, 1978.

4. Tennessee Valley Authority Division of Engineering Design, Civil Engineering Branch, Watts Bar Nuclear Plant Static and Linear Local Dynamic Internal Pressure Capability of the Steel Containment Vessel, June 12, 1981.

5. Faires, Virgil M, Design of Machine Elements, Third Edition, MacMillian Company, 1955, pp. 139-144.

6. Bathe, K. J., ADINA: A Finite Element Program for Automatic Dynamic Incremental Nonlinear Analysis, MIT Rep. 82448-1, Sept. 1975 (revised Dec. 1978).

7. Cook, W. A., Linear and Nonlinear Symmetrically Loaded Shells of Revolution Approximated with a Finite Element Method, Los Alamos Scientific Laboratory, Rep. LA-7538-MS (Oct. 1978).

8. Stone & Webster Engineering Corp., Specifications for Reinforcing Steel Maine Yankee Atomic Power Station Maine Yankee Atomic Power Company, Wiscasset, Maine, March 8, 19768, Boston, Mass.

9. Bathe, K. J. and S. Ramaswany, "On Three-Dimensional Non-linear Analysis of Concrete Structures," Mech. Engng. Design, 52, 385-409 (1979).

10. Butler, T. A. and J. G. Bennett, "Nonlinear Response of a Post-Tensioned Concrete Structure to Static and Dynamic Internal Pressure Loads," Computers and Structures, vol. 13, pp. 647-659, 1981.

11. Olyniec, J.H., "Bellefonte Primary Containment Structure," Preprint 80-548, ASCE Convention and Exposition, Florida, October. 27-31, 1980.

12. Chen, Andre and Wai F. Chen, "Constitutive Relations for Concrete," Journal of the Engineering Mechanics Division, ASCE, vol. 101, No. EM4, Proc. Paper 1529, August, 1975, pp. 465-481.

13. Cones, M. A., Bellefonte Nuclear Plant Primary Containment Analysis of Tests for Concrete Properties, TVA Engineering Report File No. 81-16, December, 1978.

## Appendix A

### Summary of Mill Test Reports Of Materials Used In the Watts Bar Containment Unit 1

**Cylindrical Shell**

| Part No. | Thickness | Yield Stress (ksi) | Tensile Strength (ksi) | Percent * Elongation |
|---|---|---|---|---|
| 52-2 | 1-3/8" | 51.3 | 77.6 | 28.5 |
| 61-1 | 1/3/8" | 44.6 | 74.2 | 27 |
| 50-4 | 1-3/8" | 44.1 | 70.7 | 25 |
| 49A | 1-3/8" | 49.2 | 76.8 | 28 |
| 49B | 1-3/8" | 45.8 | 71.2 | 33 |
| 49C | 1-3/8" | 48.5 | 75.8 | 22 |
| 58A | 1-3/8" | 46.2 | 77.0 | 24 |
| 58B | 1-3/8" | 44.9 | 73.7 | 25 |
| 58C | 1-3/8" | 42.4 | 72.7 | 29.0 |
| 87-1 | 1-3/8" | 46.3 | 70.5 | 26.0 |
| 60A | 1-3/8" | 42.4 | 72.7 | 29.0 |
| 90-1 (1) | 1-1/2" | 39.4 | 71.4 | 34 |
| 90-1 (2) | 1-1/2" | 49.3 | 72.8 | 32 |
| 90-1 (3) | 1-1/2" | 47.8 | 73.8 | 34 |
| 90-1 (4) | 1-1/2" | 49.3 | 72.8 | 32 |

* The number of significant figures are as reported in the Mill Test Reports.

Cylindrical Shell (continued)

| Part No. | Thickness | Yield Stress (ksi) | Tensile Strength (ksi) | Percent Elongation |
|---|---|---|---|---|
| 90-1 (5) | 1-1/2" | 46.5 | 75.6 | 29 |
| 90-1 (6) | 1-1/2" | 48.8 | 75.6 | 28 |
| 90-1 (7) | 1-1/2" | 44.8 | 73.4 | 35 |
| 90-1 (8) | 1-1/2" | 47.0 | 79.0 | 29 |
| 90-1 (9) | 1-1/2" | 50.0 | 75.5 | 33 |
| 90-1 (11) | 1-1/2" | 39.5 | 73.5 | 32 |
| 90-1 (12) | 1-1/2" | 44.8 | 70.7 | 34 |
| 90-1 (14) | 1-1/2" | 44.6 | 72.4 | 33 |
| 90-1 (16) | 1-1/2" | 46.1 | 75.8 | 25 |
| 90-1 (17) | 1-1/2" | 43. | 79.0 | 32 |
| Average | | 45.9 | 74.2 | 29.5 |
| Standard Deviation | | 3.07 | 2.51 | 3.68 |

Dome

| Part No. | Thickness | Yield Stress (ksi) | Tensile Strength (ksi) | Percent Elongation |
|---|---|---|---|---|
| 401-1 (2) | 1-3/8" | 42.0 | 71.0 | 32 |
| 401-1 (3) | 1-3/8" | 50.1 | 75.2 | 31 |
| 401-1 (5) | 1-3/8" | 48.6 | 75.6 | 32 |
| 401-1 (6) | 1-3/8" | 51.1 | 75.9 | 30.5 |
| 401-1 (7) | 1-3/8" | 53.8 | 74.7 | 30.0 |
| 401-1 (8) | 1-3/8" | 52.0 | 74.5 | 30.0 |

Dome (continued)

| Part No. | Thickness | Yield Stress (ksi) | Tensile Strength (ksi) | Percent Elongation |
|---|---|---|---|---|
| 401-1 (9) | 1-3/8" | 53.3 | 76.8 | 28.0 |
| 401-1 (10) | 1-3/8" | 52.4 | 74.9 | 30.0 |
| 401-1 (11) | 1-3/8" | 41.5 | 71. | 34 |
| 401-1 (12) | 1-3/8" | 47.7 | 73.5 | 25 |
| 401-1 (13) | 1-3/8" | 38.0 | 71.7 | 26 |
| 401-1 (15) | 1-3/8" | 49.4 | 77.7 | 24 |
| 401-1 (16) | 1-3/8" | 45.5 | 73.6 | 27 |
| 401-1 (17) | 1-3/8" | 45.7 | 73.7 | 25 |
| 401-1 (18) | 1-3/8" | 43.0 | 71.0 | 35 |
| 401-2 (1) | 13/16" | 48.2 | 74.0 | 24 |
| 401-2 (2) | 13/16" | 43.7 | 70.3 | 23 |
| 401-2 (3) | 13/16" | 48.2 | 72.0 | 26 |
| 401-2 (4) | 13/16" | 30.6 | 74.8 | 30 |
| 401-2 (5) | 13/16" | 44.5 | 71.4 | 29 |
| 401-2 (6) | 13/16" | 51.7 | 74.5 | 26 |
| 401-2 (7) | 13/16" | 51.8 | 75.6 | 27.1 |
| 401-2 (8) | 13/16" | 44.4 | 70.8 | 23 |
| 401-2 (9) | 13/16" | 48.5 | 73.2 | 27 |
| 401-2 (10) | 13/16" | 50.6 | 74.1 | 25 |
| 402-3 (1) | 13/16" | 52.8 | 77.2 | 28.5 |
| 402-3 (2) | 13/16" | 55.4 | 82.6 | 26.0 |

Dome (continued)

| Part No. | Thickness | Yield Stress (ksi) | Tensile Strength (ksi) | Percent Elongation(%) |
|---|---|---|---|---|
| 402.3 (3) | 13/16" | 55.4 | 82.6 | 26.0 |
| 402.3 (4) | 13/16" | 54.7 | 81.8 | 26.0 |
| 402-1 | 15/16"** | 51.9 | 76.1 | 26.0 |
| 402-2 (1) | 15/16"*** | 47.9 | 75.9 | 25.5 |
| (2) | 15/16** | 51.8 | 7 .9 | 28 |
| Average | | 46.3 | 74.8 | 27.7 |
| Atandard Deviation | | 5.35 | 3.17 | 3.06 |

Personnel Hatch Bulkhead and Hatch

| Part No. | Thickness | Yield Stress (ksi) | Tensile Strength (ksi) | Percent Elongation |
|---|---|---|---|---|
| 155-11 | 1/2" | 50.7 | 73.4 | 22 |
| 157-2 (1) | 1/2" | 50.7 | 73.4 | 22 |
| (2) | 1/2" | 50.7 | 73.4 | 22 |
| Average | | 50.7 | 73.4 | 22 |

Equipment Hatch

| Part No. | Thickness | Yield Stress (ksi) | Tensile Strength (ksi) | Percent Elongation |
|---|---|---|---|---|
| 443-1 | 3/4" | 48.4 | 76.9 | 24 |
| 443-2 (1) | 3/4" | 48.4 | 72.9 | 19.0 |

Equipment Hatch (continued)

| Part No. | Thickness | Yield Stress (ksi) | Tensile Strength (ksi) | Percent Elongation |
|---|---|---|---|---|
| 443-2 (2) | 3/4" | 48.9 | 72.9 | 19.0 |
| 443-3 | 1-1/2" | 51.8 | 81.6 | 29.0 |
| 443-4 | 1-1/2" | 51.8 | 81.6 | 29.0 |
| 443-5 | 1-1/2" | 51.8 | 81. | 29.0 |
| Average | | 50.2 | 77.9 | 24.8 |
| Standard Deviation | | 1.78 | 4.29 | 4.92 |

Tie Down Bolts

| Spec. No. | Yield Stress (psi) | Tensile Strength (psi) | Ultimate Strain |
|---|---|---|---|
| A11 | 113,250 | 135,250 | 19.5 |
| A12 | 117,250 | 138,500 | 19.0 |
| A14 | 115,500 | 137,000 | 18.5 |
| A15 | 114,000 | 136,000 | 19.5 |
| A16 | 113,750 | 136,500 | 21.0 |
| A17 | 122,750 | 140,000 | 19.0 |
| A18 | 116,500 | 136,500 | 19.0 |
| A19 | 112,250 | 135,000 | 19.0 |
| A20 | 117,000 | 138,250 | 19.0 |
| *19 | 115,000 | 135,250 | 20.5 |
| Average | 115,725 | 136,825 | 19.4 |
| Standard Deviation | 2,973 | 1,637 | 0.77 |

## Appendix B

### Summary of Mill Test Reports of the Materials Used In the Bellefonte Containment Unit 1

### Bellefonte Rebar Data

### No. 11 Reinforcing Bar

| Sample No. | Yield Stress (Psi) | Ultimate Stress (Psi) | Percent Elongation |
|---|---|---|---|
| 1 | 65,385 | 100,641 | 14.00 |
| 2 | 65,705 | 104,167 | 13.50 |
| 3 | 71,474 | 113,782 | 10.50 |
| 4 | 60,256 | 98,076 | 14.00 |
| 5 | 71,794 | 108,974 | 10.75 |
| 6 | 63,461 | 100,000 | 15.50 |
| 7 | 71,794 | 108,974 | 10.75 |
| 8 | 72,115 | 111,858 | 11.75 |
| 9 | 65,385 | 100,641 | 14.00 |
| 10 | 65,750 | 104,167 | 13.50 |
| 11 | 65,385 | 100,641 | 14.00 |
| 12 | 67,948 | 105,769 | 13.50 |
| 13 | 66,666 | 104,807 | 7.00 |
| 14 | 62,179 | 99,038 | 13.75 |
| 15 | 61,538 | 100,692 | 13.50 |
| 16 | 69,551 | 108,974 | 10.50 |
| 17 | 66,666 | 104,807 | 7.00 |
| 18 | 61,858 | 101,282 | 14.50 |
| 19 | 66,666 | 104,807 | 7.00 |
| 20 | 75,000 | 116,026 | 10.50 |
| 21 | 61,858 | 101,282 | 14.50 |
| 22 | 66,666 | 101,602 | 13.75 |
| 23 | 68,590 | 106,090 | 12.50 |
| 24 | 67,949 | 107,051 | 10.50 |
| 25 | 70,833 | 107,692 | 13.75 |
| 26 | 74,359 | 112,179 | 14.50 |
| 27 | 66,666 | 101,602 | 13.75 |
| 28 | 68,590 | 106,090 | 12.50 |
| 29 | 70,513 | 107,692 | 12.50 |
| 30 | 71,474 | 109,615 | 12.50 |
| 31 | 60,269 | 105,449 | 14.00 |
| 32 | 62,179 | 99,038 | 13.75 |

Bellefonte Rebar Data

No. 11 Reinforcing Bar Cont'd

| Sample No. | Yield Stress (Psi) | Ultimate Stress (Psi) | Percent Elongation |
|---|---|---|---|
| 33 | 60,577 | 100,000 | 13.75 |
| 34 | 71,153 | 113,782 | 8.00 |
| 35 | 61,858 | 101,282 | 14.50 |
| 36 | 68,590 | 105,769 | 15.50 |
| 37 | 71,474 | 109,615 | 12.50 |
| 38 | 66,666 | 101,923 | 14.00 |
| 39 | 72,756 | 100,576 | 9.00 |
| 40 | 73,397 | 109,935 | 11.00 |
| 41 | 68,269 | 104,487 | 12.50 |
| 42 | 69,230 | 107,370 | 10.50 |
| 43 | 63,782 | 104,166 | 13.75 |
| 44 | 72,756 | 110,576 | 9.00 |
| 45 | 72,435 | 108,012 | 14.75 |
| 46 | 66,346 | 101,602 | 9.00 |
| 47 | 68,269 | 103,525 | 13.50 |
| 48 | 63,461 | 100,000 | 15.50 |
| Average | 67,448 | 105,127 | 13.09 |
| Standard Deviation | 4,076 | 4,461 | 4.96 |

Bellefonte Rebar Data

No. 9 Reinforcing Bar

| Sample No. | Yield Stress (Psi) | Ultimate Stress (Psi) | Percent Elongation |
|---|---|---|---|
| 1 | 69,500 | 110,500 | 10.00 |
| 2 | 70,000 | 106,500 | 12.75 |
| 3 | 68,000 | 105,500 | 13.00 |
| 4 | 70,000 | 106,500 | 12.75 |
| 5 | 76,500 | 123,000 | 10.00 |
| 6 | 70,000 | 107,500 | 11.75 |
| 7 | 76,500 | 123,000 | 10.00 |
| 8 | 69,500 | 110,500 | 10.00 |
| 9 | 68,000 | 105,500 | 13.00 |
| 10 | 70,000 | 106,500 | 12.75 |
| 11 | 60,500 | 94,500 | 10.00 |
| 12 | 72,000 | [illegible] | [illegible] |
| 13 | 67,500 | 104,000 | 14.00 |
| 14 | 72,000 | 110,000 | 16.00 |
| 15 | 67,500 | 104,000 | 14.00 |
| 16 | 71,000 | 113,000 | 12.50 |
| Average | 69,906 | 108,750 | 12.15 |
| Standard Deviation | 3,693 | 6,943 | 3.20 |

BELLEFONTE REBAR DATA

No. 8 Reinforcing Bar

| Sample No. | Yield Stress (Psi) | Ultimate Stress (Psi) | Percent Elongation |
|---|---|---|---|
| 1 | 73,418 | 109,494 | 12.75 |
| 2 | 72,152 | 110,127 | 13.50 |
| 3 | 77,215 | 115,823 | 13.50 |
| 4 | 68,354 | 104,430 | 16.00 |
| 5 | 68,354 | 103,797 | 17.00 |
| 6 | 73,418 | 109,494 | 12.75 |
| 7 | 72,152 | 110,127 | 13.50 |
| 8 | 74,684 | 111,392 | 14.25 |
| 9 | 81,012 | 122,152 | 13.00 |
| 10 | 68,354 | 104,430 | 16.00 |
| 11 | 68,354 | 103,797 | 17.00 |
| 12 | 75,949 | 113,924 | 13.25 |
| 13 | 81,012 | 122,152 | 13.00 |
| 14 | 81,012 | 118,987 | 13.00 |
| 15 | 75,949 | 113,924 | 13.25 |
| 16 | 81,012 | 118,987 | 13.00 |
| 17 | 75,949 | 113,924 | 13.25 |
| 18 | 65,189 | 99,367 | 16.00 |
| 19 | 69,620 | 106,962 | 13.00 |
| 20 | 70,886 | 106,962 | 14.25 |
| 21 | 68,354 | 106,962 | 14.00 |
| 22 | 71,518 | 108,860 | 15.75 |
| 23 | 70,886 | 107,594 | 16.00 |
| 24 | 65,189 | 99,367 | 16.00 |
| 25 | 72,152 | 113,291 | 13.50 |
| 26 | 78,481 | 118,354 | 13.75 |
| 27 | 74,684 | 113,291 | 15.00 |
| 28 | 68,354 | 102,531 | 17.00 |
| 29 | 68,354 | 106,962 | 14.00 |
| 30 | 67,089 | 103,165 | 16.00 |
| 31 | 74,684 | 113,291 | 15.00 |
| 32 | 77,848 | 118,354 | 12.50 |
| 33 | 71,518 | 108,860 | 15.75 |
| 34 | 65,822 | 101,898 | 17.00 |
| 35 | 72,152 | 113,291 | 13.50 |
| 36 | 75,943 | 111,392 | 14.00 |
| 37 | 74,684 | 113,291 | 15.00 |
| Average | 72,713 | 110,297 | 14.46 |
| Standard Deviation | 4,599 | 6,033 | 1.44 |

Bellefonte Rebar Data

No. 6 Reinforcing Bar

| Sample No. | Yield Stress (Psi) | Ultimate Stress (Psi) | Percent Elongation |
|---|---|---|---|
| 1 | 61,590 | 96,363 | 16.50 |
| 2 | 66,363 | 108,636 | 13.00 |
| 3 | 67,045 | 104,090 | 15.00 |
| 4 | 73,863 | 115,909 | 10.00 |
| 5 | 71,363 | 113,636 | 14.00 |
| 6 | 72,045 | 112,954 | 11.00 |
| 7 | 63,636 | 99,545 | 15.00 |
| 8 | 66,818 | 102,727 | 14.75 |
| 9 | 67,272 | 105,000 | 11.00 |
| 10 | 71,363 | 113,636 | 14.00 |
| 11 | 64,318 | 100,681 | 15.00 |
| 12 | 66,818 | 102,727 | 14.75 |
| 13 | 60,454 | 94,409 | 16.25 |
| 14 | 71,363 | 113,636 | 14.00 |
| 15 | 67,045 | 104,545 | 13.25 |
| 16 | 69,090 | 112,272 | 11.50 |
| 17 | 72,272 | 115,227 | 12.00 |
| 18 | 60,454 | 93,409 | 16.25 |
| 19 | 72,045 | 112,954 | 11.00 |
| 20 | 64,318 | 100,681 | 15.00 |
| 21 | 66,818 | 108,409 | 12.50 |
| 22 | 69,772 | 111,136 | 12.00 |
| 23 | 73,636 | 115,227 | 10.50 |
| 24 | 67,772 | 111,136 | 12.00 |
| 25 | 72,954 | 114,772 | 10.00 |
| 26 | 63,636 | 100,454 | 15.25 |
| Average | 67,851 | 107,083 | 13.29 |
| Standard Deviation | 4,043 | 7,027 | 2.03 |

Bellefonte Equipment Hatch
Material Data

| No. | Yield Stress (Psi) | Ultimate Stress (Psi) | Percent Elongation |
|---|---|---|---|
| 1 | 51,800 | 79,400 | 29.00 |
| 2 | 52,500 | 79,000 | 29.00 |
| 3 | 49,700 | 78,500 | 30.00 |
| 4 | 51,000 | 82,500 | 29.00 |
| 5 | 51,800 | 79,400 | 29.00 |
| 6 | 51,000 | 82,500 | 29.00 |
| 7 | 49,200 | 79,000 | 30.00 |
| 8 | 49,700 | 78,500 | 30.00 |
| Average | 50,838 | 79,850 | 29.38 |
| Standard Deviation | 1,191 | 1,670 | 0.52 |

Bellefonte Personnel Lock
Material Data

| No. | Yield Stress (Psi) | Ultimate Stress (Psi) | Percent Elongation |
|---|---|---|---|
| 1 | 52,500 | 80,600 | 28.00 |
| 2 | 52,600 | 72,500 | 24.00 |
| 3 | 50,600 | 71,200 | 24.00 |
| 4 | 47,500 | 73,200 | 29.00 |
| 5 | 45,200 | 71,800 | 28.00 |
| 6 | 47,500 | 74,000 | 30.00 |
| 7 | 47,300 | 72,000 | 30.00 |
| 8 | 64,[illegible] | 72,000 | 27.00 |
| 9 | 51,200 | 73,500 | 24.00 |
| 10 | 52,000 | 76,700 | 21.00 |
| 11 | 50,000 | 70,200 | 24.00 |
| 12 | 51,000 | 75,200 | 27.00 |
| 13 | 53,200 | 79,100 | 29.00 |
| 14 | 50,800 | 76,200 | 25.00 |
| 15 | 50,300 | 75,000 | 28.00 |
| 16 | 54,200 | 77,700 | 22.00 |
| 17 | 53,900 | 76,000 | 26.00 |
| 18 | 51,000 | 76,500 | 26.00 |
| 19 | 53,000 | 75,900 | 28.00 |
| 20 | 54,000 | 76,500 | 23.00 |
| 21 | 53,900 | 77,500 | 23.00 |
| 22 | 54,000 | 75,900 | 25.00 |
| 23 | 53,800 | 76,200 | 24.00 |
| 24 | 45,600 | 70,400 | 28.00 |
| 25 | 48,900 | 76,200 | 27.00 |
| 26 | 62,000 | 83,100 | 24.00 |
| 27 | 48,600 | 70,400 | 24.00 |
| 28 | 49,600 | 71,000 | 27.00 |
| Average | 51,753 | 74,875 | 25.89 |
| Standard Deviation | 4,219 | 3,209 | 2.45 |

Bellefonte Liner Data

1/4" Liner Plate Cont'd

| Sample No. | Yield Stress (Psi) | Ultimate Stress (Psi) | Percent Elongation |
|---|---|---|---|
| 44 | 46,200 | 67,100 | 24.00 |
| 45 | 46,000 | 64,000 | 25.00 |
| 46 | 43,500 | 62,400 | 27.00 |
| 47 | 50,100 | 62,800 | 25.00 |
| 48 | 44,000 | 63,200 | 30.00 |
| 49 | 48,600 | 63,800 | 25.00 |
| 50 | 46,300 | 67,400 | 27.00 |
| 51 | 45,300 | 63,000 | 30.00 |
| 52 | 46,300 | 67,400 | 27.00 |
| 53 | 46,500 | 64,600 | 29.00 |
| 54 | 45,300 | 63,400 | 25.00 |
| 55 | 46,000 | 64,200 | 26.00 |
| 56 | 46,500 | 64,600 | 29.00 |
| 57 | 45,700 | 64,200 | 25.00 |
| 58 | 45,800 | 64,000 | 25.00 |
| 59 | 43,400 | 63,400 | 25.00 |
| 60 | 43,400 | 63,400 | 25.00 |
| 61 | 42,500 | 63,200 | 24.00 |
| 62 | 48,000 | 64,100 | 22.00 |
| 63 | 42,100 | 63,400 | 26.00 |
| 64 | 45,700 | 63,400 | 28.00 |
| 65 | 40,300 | 60,200 | 32.00 |
| 66 | 40,300 | 60,200 | 32.00 |
| 67 | 43,600 | 62,600 | 27.00 |
| 68 | 45,000 | 65,400 | 26.00 |
| 69 | 43,600 | 62,600 | 27.00 |
| 70 | 44,200 | 63,600 | 27.00 |
| 71 | 45,700 | 64,000 | 29.00 |
| 72 | 46,000 | 63,800 | 26.00 |
| 73 | 45,600 | 64,000 | 26.00 |
| 74 | 46,000 | 63,800 | 26.00 |
| 75 | 45,600 | 63,400 | 26.00 |
| 76 | 44,500 | 64,400 | 25.00 |
| 77 | 46,100 | 62,500 | 28.00 |
| 78 | 44,600 | 63,000 | 26.00 |
| 79 | 44,200 | 62,000 | 27.00 |
| 80 | 50,800 | 65,700 | 23.00 |
| 81 | 51,000 | 66,500 | 25.00 |
| 82 | 44,200 | 61,000 | 26.00 |
| 83 | 44,400 | 63,000 | 25.00 |
| 84 | 44,200 | 61,000 | 26.00 |
| 85 | 54,100 | 70,600 | 22.00 |
| Average | 45,780 | 64,313 | 26.54 |
| Standard Deviation | 2,753 | 2,211 | 2.05 |

NRC FORM 335 (11 81)

U.S. NUCLEAR REGULATORY COMMISSION

**BIBLIOGRAPHIC DATA SHEET**

1 REPORT NUMBER (Assigned by DDC)
NUREG/CR-3782

4 TITLE AND SUBTITLE (Add Volume No., if appropriate)
Geologic and Hydrologic Research at the Western New York Nuclear Service Center , West Valley, New York - Final Report, August 1982 - December 1983

2 (Leave blank)

3 RECIPIENT'S ACCESSION NO.


7 AUTHOR(S)
J.R. Albanese, S.L. Anderson, R.H. Fakundiny, S.M. Potter, W.B. Rogers, L.F. Whitbeck


5 DATE REPORT COMPLETED
MONTH November YEAR 1983


9 PERFORMING ORGANIZATION NAME AND MAILING ADDRESS (Include Zip Code)
New York State Geologic Survey/State Museum
New York State Education Department
Albany, New York 12230


DATE REPORT ISSUED
MONTH June YEAR 1984

6 (Leave blank)

8 (Leave blank)

12 SPONSORING ORGANIZATION NAME AND MAILING ADDRESS (Include Zip Code)
Division of Radiation Programs and Earth Sciences
Office of Nuclear Regulatory Research
U.S. Nuclear Regulatory Commission
Washington, D. C. 20555

10 PROJECT TASK/WORK UNIT NO.

11 FIN NO.
B6350
NRC-04-79-205

13 TYPE OF REPORT
Final

PERIOD COVERED (Inclusive dates)
August 1982 - December 1983

15 SUPPLEMENTARY NOTES Appendices by R. G. LaFleur, RPI, and J.C. Boothrogd and B. S. Tinson, Earth Surface Res., Inc.

14 (Leave blank)

16 ABSTRACT (200 words or less)


This report is the last in a series by the New York State Geological Survey on studies funded by the U.S. Nuclear Regulatory Commission. The report covers five important aspects of the geology and hydrology of the Western New York Nuclear Service Center, near West Valley, New York: geomorphology, stratigraphy, sedimentology, surface water, and radionuclide analyses. We reviewed past research on these subjects and present new data obtained in the final phase of NYSGS research at the site. Also presented are up-to-date summaries of the present knowledge of geomorphology and stratigraphy. The report contains a significant bibliography of previous West Valley studies. Appendices include a report on the Fall 1983 Drilling Project and the procedures used, history and prognosis of Cattaraugus Creek and tributaries down cutting, and bar modification and landslide processes of Buttermilk Valley.


17 KEY WORDS AND DOCUMENT ANALYSIS

17a DESCRIPTORS

17b IDENTIFIERS/OPEN-ENDED TERMS
Geology, Hydrology, Geomorphology, Stratigraphy Sedimentology, Radionuclide Analyses

18 AVAILABILITY STATEMENT
Unlimited

19 SECURITY CLASS (This report)
UNCLASSIFIED

21 NO. OF PAGES

20 SECURITY CLASS (This page)
UNCLASSIFIED

22 PRICE

NRC FORM 335 (11 81)

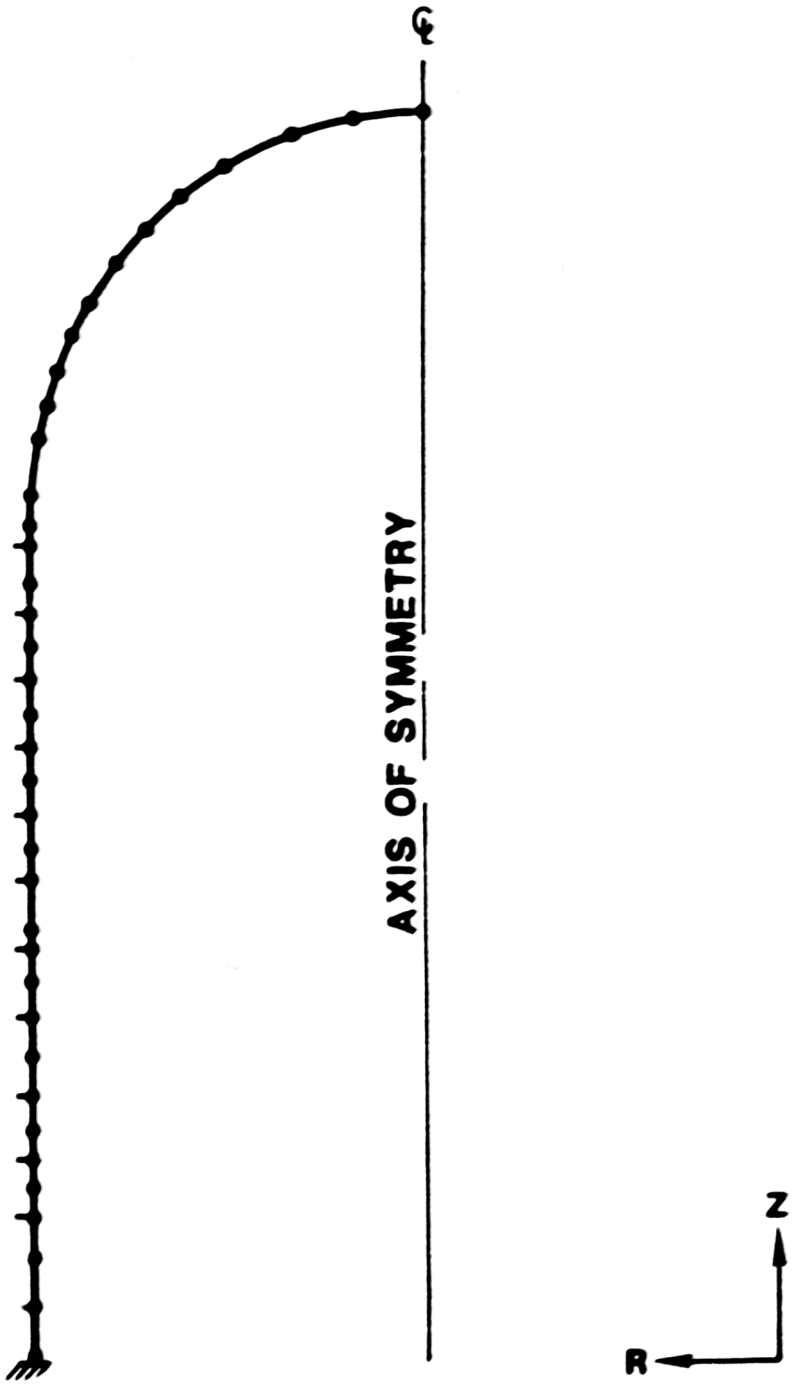


Figure 2

Axisymmetric Finite Element Model
of the Watts Bar Containment

First yielding was calculated to occur at 90 psig at the base of the containment. General yielding of the cylinder wall at mid-cylinder height occurred at approximately 120 psig (see displaced shape plot in Figure 4). Also, yielding of the dome material was quite apparent at this load. Once general yielding occurs, the containment becomes noticeably distorted, Figure 5.

The radial deflection at mid-cylinder height as a function of internal pressure is plotted in Figure 6. At 120 psig, the radial deflection is approximately 1.0 inch, while at 175 psig the deflection is over 40 inches. These computations assume that there are no restraining elements such as piping or the shield building. This, of course, is not the real case and it is unrealistic to expect that displacements of the order of 40 inches could occur before some interaction would invalidate the analysis; e.g., contact with the wall of the shield building. Nonetheless, the assumptions of the analysis leads to an upper bound ultimate strength prediction of approximately 175 psig and that failure (assuming a maximum von Mises stress criteria) would occur in the 13/16-inch dome section, Figure 7. An approximate realistic lower bound could be 120 psig at which pressure the deflections are still reasonably small. The containment shell itself could be expected to have an ultimate capacity between these two values.

## Equipment Hatch Analysis

### Equipment Hatch Description

The Watts Bar equipment hatch structure, Figure 8, consists of the shell insert, a 20-foot diameter door and twenty 1-1/4 inch diameter equally spaced swing bolts. The door is a 3/4-inch thick, 20-foot radius spherically dished section. The seals have double compression gaskets between the door tension ring and the penetration sleeve.

The equipment hatch failure mode of most interest was buckling due to the internal pressure. It is probable that buckling of the hatch door would cause large displacements of the tension ring, breaking the seal and causing a loss of pressure containment.

### Finite Element Modeling

The stress-strain curve used in the analysis was constructed from as-built material properties (Appendix A) in the same fashion as was done for the containment shell analysis.

updated current stiffness matrix, but after each load step, equilibrium between the applied and internal forces must be reestablished using either a modified Newton method or a BFGS matrix update procedure [6]. Neither of these techniques were successful in obtaining convergent solutions. This result was similar to that found in a different study using ADINA [10]. Because the ADINA program does not have a full Newton-Raphson technique capability, solutions were obtained by taking small pressure load steps of 0.1 psi and reforming the stiffness matrix at each load step. Small load steps were taken to minimize the error. This strategy was apparently successful since reasonable results were obtained.

The containment structure exhibited a linear response up to an internal pressure of 31 psig. At that pressure, severe hoop cracking occured involving essentially the entire cylindrical wall and continuing to approximately half way up the dome. The hoop forces were redistributed to the still elastic liner and hoop rebar elements. At 33 psig, the hoop cracking had progressed through the entire dome. Between 33 and 73 psig the concrete cracking progressed at a much slower rate with some additional in-plane crack development (cracks that are perpendicular to the plane of the finite element model). At 73 psig the first yielding of the liner occurred at mid-cylinder height.

As the internal pressure increased to 118 psig, additional in-plane cracks developed throughout the dome, cylinder wall, and cylinder wall-basemat intersection region. At this pressure, the liner yielding had progressed to include the entire dome region and cylinder wall to approximately 12' above the basemat. Also at 118 psig, the general yielding of the hoop reinforcing bars had begun.

The analysis ended when a numerical instability was encountered at 129 psig. This instability was probably the result of the very severe damage of the structure at the cylinder wall-basemat interface, the region associated with the instability. At this point in the analysis the concrete material of the containment building is severely damaged and general yielding of the cylinder hoop reinforcing bars and liner has already occurred.

A plot of pressure versus radial displacement at mid-cylinder height is shown in Figure 21. The loss in stiffness as the initial cylinder wall cracks developed is quite apparent at 31 psig. The yielding of the liner (beginning at 73 psig) has only a slight influence on the stiffness of the structure while the effect of the hoop reinforcing bar yielding at 118 psig is dramatic.

Bellefonte Liner Data

1/4" Liner Plate

| Sample No. | Yield Stress (Psi) | Ultimate Stress (Psi) | Percent Elongation |
|---|---|---|---|
| 1 | 51,400 | 63,200 | 26.00 |
| 2 | 41,600 | 62,300 | 25.00 |
| 3 | 43,100 | 60,300 | 26.00 |
| 4 | 40,800 | 60,800 | 26.00 |
| 5 | 42,000 | 60,400 | 26.00 |
| 6 | 42,000 | 62,200 | 29.00 |
| 7 | 44,000 | 63,000 | 24.00 |
| 8 | 44,500 | 65,200 | 26.00 |
| 9 | 51,200 | 68,000 | 22.00 |
| 10 | 49,600 | 68,400 | 27.00 |
| 11 | 50,000 | 68,300 | 28.00 |
| 12 | 44,600 | 64,200 | 28.00 |
| 13 | 48,000 | 67,400 | 28.00 |
| 14 | 44,800 | 66,000 | 29.00 |
| 15 | 46,100 | 66,000 | 30.00 |
| 16 | 47,900 | 66,800 | 27.00 |
| 17 | 47,300 | 66,200 | 25.00 |
| 18 | 47,000 | 65,600 | 27.00 |
| 19 | 45,000 | 66,600 | 27.00 |
| 20 | 45,800 | 64,700 | 25.00 |
| 21 | 45,000 | 66,000 | 24.00 |
| 22 | 46,400 | 67,400 | 24.00 |
| 23 | 43,400 | 65,700 | 28.00 |
| 24 | 45,900 | 67,000 | 26.00 |
| 25 | 44,900 | 66,400 | 25.00 |
| 26 | 45,100 | 62,200 | 28.00 |
| 27 | 43,800 | 62,000 | 26.00 |
| 28 | 50,600 | 67,200 | 30.00 |
| 29 | 43,800 | 61,600 | 27.00 |
| 30 | 50,600 | 67,200 | 30.00 |
| 31 | 44,700 | 62,400 | 26.00 |
| 32 | 47,900 | 65,000 | 26.00 |
| 33 | 47,700 | 64,200 | 25.00 |
| 34 | 47,600 | 64,700 | 26.00 |
| 35 | 49,500 | 65,300 | 26.00 |
| 36 | 49,700 | 64,100 | 27.00 |
| 37 | 44,400 | 64,100 | 26.00 |
| 38 | 47,600 | 65,900 | 27.00 |
| 39 | 49,600 | 68,400 | 27.00 |
| 40 | 46,300 | 67,000 | 28.00 |
| 41 | 43,600 | 62,600 | 27.00 |
| 42 | 45,000 | 64,100 | 28.00 |
| 43 | 40,300 | 60,200 | 32.00 |